Development of novel surface coating material with dual functionality of antibacterial activity and protein repellency

Osaka University Graduate School of Dentistry

Course for Oral Science

(Department of Biomaterials Science)

Supervisor: Professor Satoshi Imazato

Pasiree Thongthai

ACKNOWLEDGEMENT

I would like to express my deepest appreciation to my supervisor, Professor Satoshi Imazato, Chair of the Department of Biomaterials Science, Osaka University Graduate School of Dentistry, for giving me the opportunity to gain research experience, along with his warm and invaluable guidance and infinite encouragement. I received great support from him, which made my time during these years both enjoyable and memorable.

I would like to express my special regards to Assistant Professor Haruaki Kitagawa. This thesis would not have been successful without his extraordinary patience and support. I learned how to work effectively and overcome obstacles by his advice.

I am particularly grateful for the advice given by Professor Yasuhiko Iwasaki, Chair of the Department of Chemistry and Materials Engineering, Faculty of Chemistry, Materials and Bioengineering, Kansai University. All his comments and feedback have been a great help in achieving success.

I appreciate the feedback given by Professor Kazunori Ikebe, Associate Professor Ryota Nomura, and Assistant Professor Tomoko Sumitomo, which has facilitated the completion of my thesis.

I also would like to acknowledge the rich, supportive academic environment and friendly interactions provided by all teachers and friends in my department. I spent a wonderful time with all of them.

Last but not least, I am grateful to my family for their love, caring, understanding, and support, even though we could not meet so often.

Pasiree Thongthai

INDEX

GENERAL INTRODUCTION

Dental reconstructive/restorative materials with antibacterial effects can be used to treat tissue defects, thereby preventing the occurrence of secondary diseases in the oral environment because many of these diseases are caused by bacterial infections. Among these materials, resin-based materials are the most frequently used for restorative and prosthetic treatments. One of the effective techniques for incorporating antibacterial properties into these dental resins is to immobilize an antibacterial component by using a polymerizable bactericide [1]; in this approach, antibacterial components are stabilized to a carrier material by various strong chemical bonds, such as covalent bonds, and inhibit bacteria that come into contact with the material without leaching from the surface [2]. Imazato *et al*. [3] synthesized such a polymerizable bactericide—12-methacryloyloxydodecylpyridinium bromide (MDPB; Figure 1a)—by combining a quaternary ammonium compound (QAC) and methacryloyl group. The QAC group is responsible for the antibacterial activity, while the methacrylate group can copolymerize with other methacrylate monomers.

Unpolymerized MDPB shows strong bactericidal activity against oral microorganisms, rapidly killing bacteria in biofilms within a short time period [4]. Owing

to its rapid bactericidal activity at the unpolymerized stage, MDPB has been incorporated into a self-etching primer to provide cavity-disinfecting effects [5]. Thus, the world's first self-etch adhesive system for composite restorations with antibacterial effects was successfully commercialized in 2004. Recently, applications of MDPB have been expanded to other resinous materials such as a root-canal sealer [6] and cavity disinfectant [7]. Unpolymerized MDPB can penetrate deeply into dentinal tubules and exhibits strong bactericidal activity, which is expected to lead to better clinical results in endodontic and restorative treatments.

When MDPB is in a polymerized form, the antibacterial component immobilized by the polymerization of MDPB inhibits bacteria without releasing the active component from the polymer [8]. This advantage was observed in resin composite restoration both directly and indirectly by addition into fillers [3,9,10]. However, because the antibacterial effects exhibited by materials with immobilized bactericides depend on the contact inhibition of bacteria, their effectiveness can be readily reduced by coverage with salivary proteins. [11–14]. This limitation should be addressed for materials used in an oral environment because they will be inevitably exposed to salivary protein in the oral cavity.

To this end, the utilization of 2-methacryloyloxyethyl phosphorylcholine (MPC), a methacrylate monomer containing a phosphorylcholine group (Figure 1b) that can be polymerized with other methacrylate monomers [15,16], was investigated as a potential

solution to this limitation. The synthesis of MPC was inspired by the structure of cell membranes; phospholipid molecules were incorporated for superior biocompatibility (Figure 2a). In addition, the MPC polymer can reduce the adsorption of proteins because of its superhydrophilicity and the presence of water structures as a hydration layer on its surface (Figure 2b) [17–19].

Protein adsorption is the first phenomenon that occurs when synthetic biomaterials come into contact with a living organism and works as a trigger for foreign body reactions with materials from a host. In the oral cavity, the adsorption of saliva-derived protein also leads to the formation of a conditioning layer (called pellicle) prior to bacterial adhesion [20–23]. Therefore, protein repellency is beneficial for the development of materials for biomedical applications. Owing to the biocompatibility and anti-biofouling property of MPC, surface modification with MPC polymer is of a great interest for various biomedical materials, such as soft contact lenses [24], ventricular assist devices [25], and hip joints [26]. It has been reported that a surface coating composed of MPC polymer prevents microbial retention to biomedical devices [27] and also inhibits streptococcal adherence to saliva-coated hydroxyapatite discs [28]. Therefore, the reduction of salivary protein adsorption by MPC incorporation may facilitate the exposure of the antibacterial component MDPB, allowing it to come into contact with bacteria in the oral environment and enhancing the antimicrobial effects.

The water-soluble MPC can be combined with n-butyl methacrylate (BMA) (Figure 1c) to form an insoluble copolymer coating, which can be applied to the surface of resinous materials *via* hydrophobic interactions between the hydrophobic unit of BMA and resin [29–31]. Therefore, copolymers composed of MDPB and MPC can be synthesized by mixing with BMA. It is expected that copolymer coatings of MDPB and MPC would demonstrate dual effects to inhibit bacterial adherence and activity on resinous material surfaces.

OBJECTIVES AND CONTENTS

The purpose of this study was to fabricate a novel, dual-functional surface coating composed of MDPB/MPC/BMA and evaluate its protein repellency and antibacterial/anti-biofilm effects on dental resins.

In experiment 1, five copolymers containing MDPB, MPC, and BMA were synthesized and coated on dental resins, followed by an assessment of surface coating abilities. The evaluation of their inhibitory effects against protein adsorption is described in experiment 2. In experiments 3 and 4, their antibacterial and anti-biofilm effects were examined. In the latter two experiments, the longevity of the antibacterial/anti-biofilm effects was tested; thus, the bio-functionalities of the surface coating materials in terms of their antibacterial and anti-biofilm effects were examined.

EXPERIMENT 1

Synthesis of copolymers and coating of dental resins

1.1 Materials and methods

1.1.1 Synthesis of copolymers and preparation of surface coatings

MDPB was synthesized according to a previous report [32]. Briefly, 12-methacryloyloxydodecyl bromide was synthesized by the reaction of 12-bromo-l-dodecanol and methacrylic acid and then converted to MDPB by reaction with pyridine. MPC was donated by NOF Co., Ltd. (Tokyo, Japan), and BMA was purchased from FUJIFILM Wako Pure Chemical Corporation (Osaka, Japan).

The copolymer was synthesized by radical polymerization of MDPB, MPC, and BMA in ethanol using 2,2'-azobisisobutyronitrile (AIBN) as an initiator (Figure 3). MDPB, MPC, and BMA at five different mole ratios of 0/30/70, 5/25/70, 15/15/70, 25/5/70, and 30/0/70 (weight ratios of 0/47/53, 11/38/51, 30/22/48, 47/7/46, and 55/0/45, respectively) were dissolved in ethanol to prepare a polymerization solution of 1 mol/L monomer concentration. Each copolymer and composition is described in Table 1. AIBN (0.5 mol%) was added to the mixture of monomers in a solution reactor, and Ar gas was

passed through the reactor for 15 min to eliminate oxygen prior to use. The mixture of monomers was stirred at 60°C for 15 h in a silicone oil bath. After diluting the polymerization solution with ethanol, unreacted monomer and polymerization initiator were removed by reprecipitation with a mixed solvent composed of diethyl ether/chloroform in a ratio of 3:2 by volume. The copolymer was filtered and dried in a desiccator overnight and obtained as the white crystalline powder (Figure 4a).

Five types of coating were prepared by dissolving each copolymer in ethanol and adjusting their concentrations to 0.5 wt%. The powders of all five groups could be dissolved thoroughly in ethanol (Figure 4b).

1.1.2 Synthesis of fluorescence-conjugated copolymers and preparation of surface coatings

For the tests to evaluate coating ability, a fluorescent monomer unit was introduced into copolymers according to a previous study [33]. MDPB, MPC, BMA, and fluorescein *O*-methacrylate (Sigma-Aldrich, St. Louis, MO, USA) at five different mole ratios of 0/30/69.5/0.5 (f-D0/C30), 5/25/69.5/0.5 (f-D5/C25), 15/15/69.5/0.5 (f-D15/C15), 25/5/69.5/0.5 (f-D25/C5), and 30/0/69.5/0.5 (f-D30/C0) were dissolved in ethanol to prepare a 1 mol/L polymerization solution. The fluorescein-conjugated copolymer (f-copolymer) was synthesized by using a free-radical polymerization technique with AIBN

as described in section 1.1.1. Subsequently, f-copolymer solution was prepared by dissolution in ethanol and adjusting the concentration to 0.5 wt% in a dark room.

1.1.3 Preparation of resin discs

A mixture of powder and liquid of PMMA (UNIFAST III clear, GC, Tokyo, Japan) at powder/liquid ratio of 2 g/mL was placed in a silicone mold with a diameter of 10 mm and thickness of 2 mm, which was pressed with a celluloid strip and a glass slide and stored for 24 h at 25°C. The cured PMMA disc was polished with wet silicon carbide paper grit 120/P120 and grit 320/P400 (CarbiMet, Buehler, Illinois, USA). Subsequently, the specimen was sterilized by ethylene oxide at 40°C for 24 h.

To prepare the cured resin composite discs, a resin composite paste (Clearfil Majesty ES Flow, Kuraray Noritake Dental, Tokyo, Japan) was placed in the silicone mold with a diameter of 10 mm and thickness of 2 mm. The surface was covered with celluloid strips and a glass slide, cured for 40 s with a light activation unit (Quick Light VL-1, Morita, Kyoto, Japan), and polished as described above.

1.1.4 Evaluation of surface coating ability

To confirm the coating of the copolymer on the resins, the PMMA or resin composite disc was immersed in 1 mL of each f-copolymer solution for 10 s and then dried for 30 min at

25°C in a dark room. These immersion and drying procedures were repeated twice. The coated surface was visualized using a fluorescence microscope with 10× magnification (TE2000 and Coolsnap cf, Nikon, Tokyo, Japan). The color images were converted to white and black, and the gray values of each image (8-bit, 256 grays scales) were analyzed using ImageJ software (National Institutes of Health, Bethesda, MD, USA) to quantify the fluorescence intensity.

1.1.5 Contact angle measurements

The PMMA disc was immersed in 1 mL of each copolymer solution for 10 s, and then the coated disc was dried for 30 min at 25°C. These immersion and drying procedures were repeated twice. The dynamic contact angles for the coated surface were recorded by an FT-125 goniometer (First Ten Angstroms, USA) with Gilmont syringes using water (deionized to 18.2 MΩ) as the probe fluid. The advancing (θA) and receding (θR) contact angles were measured by water drop addition and withdrawal, respectively. The experiments were repeated five times. The statistical data was conducted by IBM SPSS Statistics 25 (SPSS Inc, Chicago, IL, USA) using one-way analysis of variance (ANOVA) and Tukey's honestly significant difference (HSD) test with a significance level of $p < .05$.

1.2 Results

1.2.1 Surface coating ability

Figure 5a shows the fluorescence microscopy images with fluorescence intensity of the PMMA surface coated with f-copolymers. The bare PMMA (control) surface exhibited weak fluorescence (fluorescent intensity = 70.9) attributed to the autofluorescence of PMMA. On the contrary, all coated specimens showed much brighter fluorescence (fluorescent intensity = 162.1–162.8), indicating that each copolymer was successfully coated on the PMMA surface.

For the resin composites (Figure 5b), the fluorescence of all coated surfaces (fluorescent intensity = 99.9–131.2) was brighter than the bare resin composites surface (control) (fluorescent intensity = 53.5), suggesting that the f-copolymers were successfully coated. Although the fluorescence on the coated resin composites was weaker than the coated PMMA surfaces, it was obvious compared to the bare resin composites and similar among all groups.

1.2.2 Contact angles

Figure 6 shows the contact angle on the surface of the PMMA coated with copolymers. For greater MPC ratios, a significantly smaller advancing contact angle was observed

(Figure 6a), which confirmed the hydrophilicity of MPC. In addition, MPC-containing groups (*i.e*., D0/C30, D5/C25, D15/C15, and D25/C5) demonstrated smaller receding contact angles than that exhibited by non-MPC (*i.e*., D30/C0) and the control group ($p < .05$, ANOVA and Tukey's HSD test) (Figure 6b).

1.3 Discussion

Several studies have focused on the incorporation of MDPB in dental restorative materials, such as a resin adhesive system and prepolymerized resin filler, which demonstrated antibacterial effects after curing [9,10,34]. However, since the antibacterial effects of resinous materials with immobilized MDPB depend on contact inhibition of bacteria, their effectiveness in an oral environment can be reduced by coverage with salivary protein [13]. On the other hand, the polymer surface coated with copolymer composed of MPC and BMA has been reported to exhibit protein repellency and inhibition of bacterial adherence [15]. In this study, MDPB was copolymerized with MPC to provide a dual functionality of protein repellency and antimicrobial activity. Zhang *et al.* [35–41] developed a dental adhesive, resin composite, and cement by simply mixing MPC polymer with an antibacterial QAC-based monomer, which inhibited oral biofilms on the surface. However, a copolymer coating composed of antibacterial monomer and MPC has not yet been reported. The surface coating was preferred over the previous

procedure of direct mixing in order to increase the surface density of exposed functional polymers. Here, a novel, dual-functional copolymer composed of MDPB and MPC was fabricated and fully dissolved in ethanol to prepare the coating solution, which can be applied to the surface of various methacrylate resins for restorative and prosthodontic materials.

In the fluorescence microscopy images, clear fluorescence was observed on the PMMA surface coated with fluorescein-conjugated D0/C30, which contained only MPC and whose structure was similar to the coating reported in the previous study [42]. It was revealed that although MPC is water soluble, when combined with BMA, insoluble copolymer can be stably bound to the PMMA surface *via* hydrophobic interactions between BMA moieties and PMMA [29–31]. In this study, the fluorescence observed on the images was associated with copolymer obtained from the copolymerization process. Our results indicated that PMMA coated with f-copolymers containing MDPB also exhibited clear fluorescence, suggesting that the BMA unit contributed to the binding interactions with PMMA even though MDPB was involved in the coated surfaces (Figure 7).

To confirm the coating ability of f-copolymers on the resin composites, a commercial resin composite (Clearfil Majesty ES Flow, super low), which contains 68 vol% silica and barium glass fillers, was used. The fluorescence brightness of the f-

copolymer-coated composites was reduced as a result of the lower amount/surface area of organic components compared to those in the PMMA resin without fillers. However, the coated composites still exhibited brighter fluorescence than the bare resin composite. This suggested that the binding ability of all surface coatings *via* hydrophobic interactions was mainly effective for organic components. These hydrophobic interactions allow for coating of the surface by a simple dipping method rather than other surface modification methods such as plasma treatment and grafting by irradiation techniques. Compared with plasma treatment or grafting techniques, this dipping approach is easier, repeatable, and the desired properties can be reproduced [30,43].

MPC is known as a polymer that prevents protein adsorption on account of its superhydrophilicity originating from the phospholipid layer [17,19,44]. Here, the hydrophilicity of surface coatings was investigated by determining the contact angles. It was found that the copolymer coatings with a greater ratio of MPC showed enhanced hydrophilicity. In particular, the advancing contact angles decreased with increasing MPC ratio. Since the copolymer coatings contained 70 mol% BMA, which would increase the hydrophobicity of the coating surfaces, no significant difference in the advanced contact angle was observed between D15/C15 and uncoated groups [45]. Nevertheless, the receding contact angles of the surfaces coated with copolymers containing ≥15% MPC were significantly decreased compared with the uncoated group. It can be inferred that

the decrease in contact angles arose from the high hydrophilicity of MPC, which would cause a reduction in the adsorption of proteins.

1.4 Summary

Novel coatings composed of MDPB, MPC, and BMA were successfully fabricated in various composition ratios. By simple dipping in the copolymer solution, it was confirmed that these coatings could be effectively coated on the surface of dental resins through hydrophobic interactions with the BMA units.

EXPERIMENT 2

Evaluation of protein adsorption to the copolymer-coated resins

2.1 Materials and methods

2.1.1 Adsorption of bovine serum albumin

Bovine serum albumin (BSA; Thermo Fisher Scientific Inc., Kanagawa, Japan) was dissolved in 0.01 mol/L phosphate buffer saline (PBS, pH 7.2–7.4, Wako Pure Chemical Corporation, Osaka, Japan) and adjusted to 4.5 g/L. The copolymer-coated PMMA specimen with a diameter of 10 mm and thickness of 2 mm, as prepared in section 1.1.3, was immersed in 1 mL BSA solution for 2 h at 37°C, and then irrigated with 1.5 mL PBS by centrifugation at 300 rpm for 5 min to remove loosely bound protein on the surface. The irrigation was repeated three times. The specimen was ultrasonicated in 1% sodium dodecyl sulfate (SDS) in PBS for 20 min to collect the adsorbed protein. The concentration of BSA was determined by using a Micro BCA Protein Assay Kit (Thermo Fisher Scientific Inc.). Briefly, 150 μL of protein solution was mixed with 150 μL of a solution containing alkaline tartrate–carbonate buffer, bicinchonic acid, and copper sulfate. After storing the specimen at 37°C for 2 h, the absorbance was measured by a microplate reader (iMark Microplate Absorbance Reader, Bio-Rad, Hercules, CA, USA)

at 560 nm, and the amount of protein was determined by the equation of the line generated in the BSA standard curve (Figure 8a). The experiments were repeated five times. A statistical analysis of the data was conducted by IBM SPSS Statistics 25 using one-way ANOVA and Tukey's HSD test with a significance level of $p < .05$.

For visualization of protein adsorption, FITC-conjugated BSA (FITC-BSA; Sigma-Aldrich) was used to evaluate the protein adsorption on the PMMA coated with copolymer (D0/30, D15/C15, D30/C0). FITC-BSA was dissolved in PBS and adjusted to 4.5 g/L. The specimen was immersed in 1 mL of FITC-BSA solution for 2 h at 37°C under dark conditions, and then irrigated by shaking in 1.5 mL PBS. The surface of each disc was observed with a fluorescence microscope (TE2000 and CoolSNAP cf) with 10× magnification (Figure 8b).

2.1.2 Adsorption of human saliva protein

Unstimulated human saliva was collected from three healthy donors at 25–35 years of age, as approved by the Ethics Review Committee of Osaka University Graduate School of Dentistry and Osaka University Dental Hospital (approval number R1-E52), and was filtered twice with a 0.22 μm syringe filter. The copolymer-coated PMMA specimen was immersed in 1 mL of filtered human saliva for 2 h at 37°C, and then irrigated with 1.5 mL PBS by centrifugation at 300 rpm for 5 min. The irrigation was repeated three times.

The specimen was ultrasonicated in 1% SDS in PBS for 20 min to collect the adsorbed protein. The concentration of salivary protein was determined by using a Micro BCA Protein Assay Kit, as described in section 2.1.1 (Figure 8a). The experiments were repeated five times. A statistical analysis of the data was conducted by IBM SPSS Statistics 25 using one-way ANOVA and Tukey's HSD test with a significance level of $p < .05$.

2.2 Results

2.2.1 BSA protein adsorption

Figure 9a shows the amount of BSA adsorbed on the surface of each specimen. After immersion in BSA solution for 2 h, the amount of BSA adsorbed on copolymers containing ≥15% MPC (*i.e.,* D0/C30, D5/C25, and D15/C15) was significantly smaller than that on the control specimen. The protein adsorption of the copolymer coating containing less than 15% MPC (*i.e.*, D25/C5 and D30/C0) was not significantly different from that of the control specimen ($p < .05$, ANOVA and Tukey's HSD test).

Figure 9b reveals the FITC-BSA adsorbed on each copolymer coating. The copolymer without MPC (*i.e.,* D30/C0) and control groups exhibited bright fluorescence, indicating more BSA protein adsorption than that of MPC-containing coatings (*i.e.,*

D0/C30, D15/C15), which revealed darker fluorescence.

2.2.2 Salivary protein adsorption

Figure 9c shows the adsorption of human salivary protein. The tendency of salivary protein adsorbed on the surfaces was consistent with the BSA adsorption for the copolymer containing ≥15% MPC (*i.e.,* D0/C30, D5/C25, and D15/C15), which exhibited a significantly smaller amount of adsorbed BSA protein, whereas D25/C5 and D30/C0 were not significantly different from the control ($p > .05$, ANOVA and Tukey's HSD test).

2.3 Discussion

The protein adsorption on materials for biomedical applications is the crucial factor in the interaction between polymeric materials and body fluids. When a material comes into contact with a fluid, nonspecific protein adsorption occurs on the material's surface and acts as a mediator for various cell responses. Therefore, the prevention of protein adsorption is a promising strategy for improving their biocompatibility [46–49]. Many studies investigating protein adsorption on biomaterial surfaces have been reported, and some methods to reduce protein adsorption also have been discussed [50]. Among them, reduced protein adsorption as a result of increasing the hydrophilicity of polymer surfaces has been reported [51,52].

Once a hydrophobic material surface like PMMA is surrounded by aqueous media such as blood or saliva, water molecules bind to the hydrophobic part of the polymer through van der Waals forces [53]. When a protein molecule is adsorbed on a polymer surface, water molecules between the protein and polymer need to be replaced, and a protein conformational change is induced to expose the hydrophobic part to the outside [54–57]. Thus, the protein contacts the polymer surface directly *via* hydrophobic interactions (Figure 10a). The protein behavior also depends on the structure of water around the polymer surface in the hydration state. Ishihara *et al*. [58] determined the conformational change in proteins adsorbed on hydrated polymers. It was found that BSA protein had no significant conformational change when it was adsorbed on MPC copolymer, whereas the changes in the α-helix content were detected on poly(2-hydroxyethyl methacrylate) (HEMA). The study on water state in the hydrated polymer revealed that polymers with hydroxyl groups, like poly(HEMA), would form a network structure of water molecules. This structure trapped a protein and prolonged the contact of the protein to the absorbed surface, subsequently leading to a conformational change in the protein [18]. On the contrary, a water-soluble MPC polymer did not disrupt hydrogen-bond formation among the water molecules, so water molecules were almost the same as pure liquid water, leading to highly mobile free water as the hydration layer around the MPC polymer [59,60]. Thus, the MPC-coated surface is similar to an aqueous

solution, so protein does not need to release bound water molecules, and the hydrophobic interaction does not occur between proteins and the polymer surface [61] (Figure 10b). In other words, the large amount of free water around the phosphorylcholine groups in MPC causes the detachment of proteins and the reduction of their adsorption [62].

Protein adsorption on the surfaces can occur rapidly when the materials come into contact with body fluids such as blood, synovial fluid, or tears. Therefore, the reduction of protein adsorption by MPC has a great benefit on the design of biocompatible interfaces for various biomedical materials. MPC is effective in suppressing platelet adhesion and activation in cardiovascular and blood-contacting devices, such as hemodialysis membranes [63], vascular prostheses [64], stents [65], cardio pulmonary bypass devices [66], and ventricular assist devices [25]. MPC has also been used in artificial hip joints to increase the surface lubrication in synovial fluid, which contains proteins, lipids, and sugar [26]. Additionally, MPC was introduced into soft contact lenses to improve oxygen permeability and wettability [24].

In this study, MPC was utilized to reduce protein adsorption on a surface surrounded by human saliva, which contains various proteins. Here, BSA (67 kDa) was selected as the model protein before using human saliva, which is more variable and complicating [67]. BSA is suitable for adsorption studies because of its high stability, availability, low cost, and high solubility in water. BSA has been widely used in studies

of protein–surface interactions and protein adsorption on phosphorylcholine-based surfaces [68–70]. The results indicated that PMMA coated by a copolymer containing ≥15% MPC inhibited the adsorption of BSA compared with uncoated PMMA. Copolymers with greater ratios of MPC (*i.e.*, D0/C30 and D5/C25) showed less BSA adsorption than that on D15/C15. It can be inferred that the high hydrophilicity of MPC, confirmed by a decrease in the contact angles on the surface, can reduce the adsorption of BSA in experiment 1.

Human saliva is a complex mixture of oral fluids, including secretions of the major and minor salivary glands and constituents of non-salivary origin derived from gingival crevicular fluid, serum and blood cells from oral wounds, oral bacteria, and desquamated epithelial cells. In this study, unstimulated saliva collected from donors was filtered with a 0.22 μm syringe filter to remove cells and bacteria. After filtration, a complex hypotonic aqueous solution remained, which contained various salivary proteins. More than 2000 proteins with different molecular weights (*e.g.,* α-amylase, 58 kDa; cystatin, 16-17 kDa; and lactotransferrin, 80 kDa [71]) and isoelectric points have been identified in saliva collected from healthy donors [72–75]. Thus, the adsorption of various proteins can be evaluated by the use of human saliva. The results of the salivary protein adsorption test revealed that PMMA coated by copolymer containing ≥15% MPC showed greater protein repellency than uncoated PMMA, similar to the case of BSA. Therefore,

the copolymer coatings composed of ≥15% MPC could inhibit nonspecific protein adsorptions on the surface of PMMA with no difference among D0/C30, D5/C25, and D15/C15. For BSA adsorption, D15/C15 showed greater protein adsorption than the other two groups. The isoelectric point of BSA is around pH 4.5–5. With raised pH, the amount of negatively charged groups in BSA increases [76]. In this study, BSA was dissolved in PBS at pH 7.2–7.4 and resulted in a negatively charged surface, which was attracted by the positive charge of the cationic portion of MDPB through electrostatic affinity [77].

2.4 Summary

Due to the hydrophilicity of the MPC polymer, the copolymer composed of ≥15% MPC could inhibit the adsorption of BSA and salivary protein on the hydrophobic surface of PMMA.

EXPERIMENT 3

Evaluation of antibacterial effects of the copolymer-coated resins

3.1 Materials and methods

3.1.1 On-disc culture assay

Streptococcus mutans NTCT10449 was used to evaluate the antibacterial activity. Stock culture was stored with Microbank vials (PRO-LAB Diagnostic, Richman Hill, ON, Canada) and stored at –80˚C. Bacteria was grown in Brain Heart Infusion (BHI; Becton Dickinson, Sparks, MD, USA) broth with 1% sucrose for 24 h at 37˚C and adjusted to approximately 1×10^6 colony-forming units (CFU)/mL.

For this test, the PMMA disc was prepared using the same method described in section 1.1.3. Then, a cylindrical cavity well (7 mm diameter and 1 mm depth) was drilled into this PMMA disc using a cylindrically shaped carbide bur mounted in a low-speed handpiece. The specimen was sterilized by ethylene oxide at 40°C for 24 h. The disc with well was immersed in 1 mL of each coating solution for 10 s, and then the coated disc was dried for 30 min at 25°C. These immersion and drying procedures were repeated twice.

To evaluate the growth of bacteria on the surface of copolymer-coated PMMA,

20 μL of *S. mutans* suspension was inoculated into the well of the five different coated discs and the control. After incubation at 37°C for 24 h, the inoculated disc was transferred to 9.98 mL BHI broth and vigorously shaken to collect the bacteria from the surface. The suspension was serially diluted, and an aliquot of the suspension was spread on a BHI agar plate (Becton Dickinson). After anaerobic incubation at 37°C for 48 h, the number of colonies was calculated (Figure 11). The experiments were repeated five times. Statistical analysis of the data was conducted by IBM SPSS Statistics 25 using one-way ANOVA and Tukey's HSD test with a significance level of $p < .05$.

To confirm whether the antibacterial effect of the coated specimen was derived from elution of the MDPB monomer, each coated resin was immersed in 1 mL of distilled water. After storage at 37˚C for 24 h, a sample volume of 500 μL was collected, and the concentration of MDPB was measured by a high-performance liquid chromatograph (HPLC; Prominence; Shimadzu, Kyoto, Japan) using a reverse-phase column (Puresil 5μ C18; Waters, Millford, MA, USA). A mixture of acetonitrile and 5 mM PBS containing 100 mM sodium perchlorate (70:30, v/v) was used as the mobile phase at a flow rate of 1 mL/min. Absorbance readings were taken at 260 nm. The minimum detectable concentration of MDPB was 0.5 μg/mL. The experiments were repeated three times.

3.1.2 Evaluation of longevity of antibacterial effects

The longevity of the antibacterial effects was evaluated on three copolymer groups: D0/C30, D15/C15, and D30/C0. The copolymer-coated PMMA disc with well was immersed in 500 μL of distilled water at 37°C for 28 days and subjected to the on-disc assay described in section 3.1.1. The experiments were repeated five times. Statistical analysis of the data among the groups was conducted by IBM SPSS Statistics 25 using ANOVA and Tukey's HSD test with a significance level of $p < .05$. The data within a group between before and after ageing was analyzed using Student's *t*-test with a significance level of $p < .05$.

3.2 Results

3.2.1 Antibacterial effects by on-disc culture assay

The number of viable *S. mutans* after incubation for 24 h on copolymer-coated and control specimens is shown in Figure 12. On the control specimen, the number of viable bacteria increased during 24-hour incubation from the initial bacterial number ($\approx 2 \times 10^4$ CFU; 4.30 $\log_{10}$CFU) to 7.00 $\log_{10}$CFU. For the copolymer coatings containing <15% MDPB (*i.e.*, D0/C30 and D5/C25), the number of bacterial cells increased to 6.91 $\log_{10}$CFU and 6.90 $\log_{10}$CFU, respectively. In contrast, the copolymer coatings containing ≥15% MDPB

(*i.e.*, D15/C15, D25/C5, and D30/C0) reduced the number of bacteria to 3.25 $1og_{10}$CFU, 3.93 $1og_{10}$CFU, and 3.39 $1og_{10}$CFU, respectively (Figure 12a). The bacterial number of the specimens coated by copolymers containing ≥15% MDPB exhibited a significantly smaller number than those on the control specimen and specimens coated by copolymers containing <15% MDPB ($p < .05$, ANOVA and Tukey's HSD test).

The HPLC analysis confirmed no elution of MDPB for all coated specimens after immersion in distilled water for 24 h.

3.2.2 Longevity of antibacterial effects

The number of viable *S. mutans* after 24-hour incubation of the specimens after 28-day immersion in distilled water is shown in Figure 12b. The number of viable cells on the specimen coated by D0/C30 increased to 6.88 log_{10}CFU, whereas the bacterial numbers of the specimens coated by D15/C15 and D30/C0 were reduced from the initial bacterial number (4.30 log_{10}CFU) to 3.19 log_{10}CFU and 3.11 log_{10}CFU, respectively. The number of viable bacteria on the specimens coated by copolymers containing ≥15% MDPB exhibited a significantly smaller number than the control specimen and specimens coated by D0/C30 without MDPB ($p < .05$, ANOVA and Tukey's HSD test).

A comparison of the number of viable *S. mutans* after incubation between before and after ageing is shown in Figure 12c. The antibacterial effect of the copolymer-coated

disc was not attenuated after the aging process, which was shown by no significant difference in the number of viable bacteria for both D15/C15 and D30/C0 between, before, and after ageing ($p > 0.05$, Student's *t*-test).

3.3 Discussion

The antibacterial activity of MDPB has been investigated in several studies. MDPB rapidly kills bacteria before curing due to the free movement of its active component, which comes into contact with bacteria. This active component is a quaternary ammonium compound; it has been suggested in various studies that the mechanism of antibacterial action is associated with the interaction between the positive charge of the ammonium cation and negative charge of the bacterial membrane. Subsequently, the electrical balance of the bacterial cell is disrupted, causing bacteriolysis [78,79]. As this is a nonspecific action, a wide range of microbes are susceptible to QAC—not only bacteria, but yeast and lipid-containing viruses [80–82]. MDPB was also found to have an antibacterial effect against various oral microbes, including cariogenic bacteria and endodontic bacteria [83–85]. Thus, MDPB has been used in various types of dental materials [6–8,86,87]. However, its antibacterial activity is reduced after curing due to the limited molecular movement caused by immobilization [8].

In this study, the bacterial number of the specimens coated by copolymers

containing ≥15% MDPB is smaller than the control specimen and specimens coated by non-MDPB-containing copolymers. The log reduction of the *S. mutans* suspension inoculated on these MDPB-coated specimens was more than 3.07–3.75 compared with that of the control specimen. Moreover, the copolymer coatings containing ≥15% MDPB reduced the bacterial number from its initial value of 4.30 $\log_{10}$CFU to 3.11–3.19 $\log_{10}$CFU (*i.e.*, 1.11–1.19 log reduction), indicating bactericidal activity on the surface. In addition, it was confirmed that no MDPB was detected in distilled water by the analysis using HPLC, suggesting the antibacterial effect did not come from the elution of unpolymerized MDPB but immobilized MDPB.

During the past two decades, Imazato *et al*. intensively investigated the antibacterial effect of various resin-based dental materials incorporating MDPB, such as adhesives and resin composites, which have been shown to demonstrate bacteriostatic effects after curing [2]. A dentin primer containing 5 wt% MDPB for a self-etch adhesive system can kill oral bacteria rapidly based on the antibacterial mechanism of action employed by unpolymerized MDPB [3]. It also has the ability to inhibit *S. mutans* after curing; however, the log reduction of *S. mutans* suspension inoculated on the cured surface after 24-hour incubation was 0.21 compared to control primer without MDPB [88]. In addition, the log reduction from the initial bacterial number was only 0.40, indicating a lower bactericidal effect than the copolymer coatings containing ≥15%

MDPB.

A resin composite containing MDPB-immobilized filler, in which the final concentration of MDPB was 2.83 wt%, inhibited bacterial growth [9]. A cured adhesive resin containing MDPB at 2.5 wt% also demonstrated a smaller number of recovered bacteria compared to commercially available adhesive resin [89]. However, these materials demonstrated a bacteriostatic rather than bactericidal effect, even though saliva treatment on their surface was not conducted before antibacterial tests. In this study, the stronger antibacterial activity can be attributed to the large concentration of MDPB in the experimental coatings (D15/C15 and D30/C0 incorporating MDPB at 30 wt% and 55 wt%, respectively). Additionally, the incorporation of MDPB directly into the materials by polymerization of MDPB or MDPB-immobilized filler might prevent the exposure of MDPB, whereas the coating on the materials was effectively exposed on its surface. Thus, the surface coating composed of a high concentration of MDPB could efficiently expose the antibacterial component on the material surface.

After aging in distilled water, the antibacterial activities of D15/C15 and D30/C0 were at the same level as those before aging. This result indicated that the coating by hydrophobic interactions was stable enough, even after aging. A previous study also reported that a copolymer of BMA and MPC coating on polyvinylidene fluoride membrane was durable after ultrasonic cleaning with SDS solution [29], thus it is possible

to clean a coated restoration by ultrasonication. This dipping method is simple, repeatable, and able to provide a prolonged period of antibacterial activity with durability, which are benefits for improving oral cavity restoration.

3.4 Summary

The copolymer coating containing ≥15% MDPB exhibited bactericidal effects. The long-lasting antibacterial effects were obtained when incubated on the specimens coated with copolymer containing ≥15% MDPB, even after 28-day aging, due to its contact killing of bacteria.

EXPERIMENT 4

Evaluation of anti-biofilm effects of copolymer-coated PMMA surface

4.1 Materials and methods

4.1.1 Biofilm formation on copolymer-coated resin

A transparent PMMA disc with a diameter of 10 mm and thickness of 1 mm (Comoglas, Kuraray, Tokyo, Japan) was purchased. The disc was coated with D0/C30, D15/C15, and D30/C0 by immersion in 1 mL of each coating solution for 10 s, and then the coated disc was dried for 30 min at 25°C. These immersion and drying procedures were repeated twice. To prepare the specimen after aging, each copolymer-coated PMMA disc was immersed in 500 μL of distilled water at 37°C for 28 days.

The copolymer-coated PMMA specimen was immersed in 1 mL of filtered human saliva described in 2.1.2 for 2 h at 37°C and then irrigated with 1.5 mL PBS by centrifugation at 300 rpm for 5 min. The irrigation was repeated three times. Subsequently, each specimen was placed in a 1.5 mL suspension of *S. mutans* NCTC 10449 in BHI with 1% sucrose adjusted to approximately 1×10^6 CFU/mL in a 24-well microplate. After anaerobic incubation at 37°C for 6 h with shaking at 100 rpm, the specimen was transferred to a new well with 1.5 mL of fresh bacterial suspension with 1% sucrose

(approximately 1 × 10^6 CFU/mL) and was anaerobically incubated. After 18 h, the specimen was again transferred to a new well with fresh bacterial suspension with 1% sucrose and further incubated for 24 h. (Figure 13)

4.1.2 Evaluation of biofilms formed on the copolymer-coated resin

To evaluate bacteria adhered on the copolymer-coated disc, the specimen with formed biofilm was irrigated twice in 1 mL of PBS with gentle shaking. The fixation and dehydration of biofilm on specimens were conducted by immersion in 0.2 M cacodylic acid for 20 min, 0.1 M half-Karnovsky's solution (glutaraldehyde and formaldehyde) for 30 min, 0.1 M cacodylic acid for 45 min, ethanol in increasing concentration (50%, 70%, 80%, 90%, and 96%) for 20 min in each concentration, and 99.5% ethanol for 90 min. After freeze-drying (JFD-320 freeze dryer, JEOL, Tokyo, Japan) for 1 h, the upper surface was sputter-coated with gold (SC-701CT, Sanyu electron, Tokyo, Japan) and observed using a scanning electron microscope (SEM; JSM-6390BU, JEOL) at 1000× magnification.

For evaluating the viability of bacteria in biofilm and the thickness of biofilm, the specimen was irrigated twice by gentle shaking in 1 mL of PBS, and the biofilm on the surface was stained using LIVE/DEAD BacLight bacterial viability kits (L7007, Molecular Probes, Eugene, OR, USA) according to the manufacturer's instruction.

Briefly, 3 μL of component A (SYTO 9 dye, 1.67 mM/propidium iodide, 1.67 mM in DMSO) and 3 μL of component B (SYTO 9 dye, 1.67 mM/ propidium iodide, 18.3 mM in DMSO) were mixed in 1 mL of distilled water. Fifty μL of the mixed solution was dropped on the specimen and incubated at 37°C for 15 min under dark conditions. After gently irrigating with distilled water, the biofilm on the specimen was visualized by a confocal laser scanning microscope (CLSM; LSM 700, Carl Zeiss, Oberkochen, Germany) with 488 and 553 nm wavelengths for excitation, and 520 and 568 nm wavelengths for emission. The image was analyzed by ZEN (Carl Zeiss, Oberkochen, Germany) and Imaris software (Bitplane, Zurich, Switzerland) to determine the thickness of biofilm and the percentage of dead cells, respectively. Statistical analysis of the data was conducted by IBM SPSS Statistics 25. The ANOVA and Tukey's HSD test were used to analyze difference of the thickness and the percentage of dead bacteria among groups with a significance level of $p < .05$. The thickness and the percentage of dead bacteria within groups between before and after aging was analyzed by the Student's *t*-test with a significance level of $p < .05$.

4.2 Results

4.2.1 Bacteria adherence on the copolymer-coated disc

Figure 14 shows the SEM images, which indicate the bacterial attachment on the coated surface after 48-hour incubation. MPC-containing copolymers (*i.e.*, D0/C30 and D15/C15) exhibited a smaller number of adhered bacteria in the form of individualized cells or small aggregations compared to that of the control and D30/C0, which showed a greater number of bacteria arranged in large clumps.

4.2.2 Viability of bacteria and thickness of biofilm

Figure 15a shows the CLSM images of specimens coated by each copolymer group after 48-hour incubation. The copolymers containing MPC (*i.e.*, D0/C30, D15/C15) exhibited thinner biofilm formation compared to that exhibited by D30/C0 and the control. By imaging analysis using ZEN software, the copolymers containing MPC (*i.e.*, D0/C30 and D15/C15) exhibited significantly thinner biofilm than D30/C0 and the control (p <.05, ANOVA and Tukey's HSD test) (Figure 15b). CLSM images and the imaging analysis using Imaris software shows that MDPB-containing copolymers (*i.e.*, D15/C15 and D30/C0) demonstrated stronger red color, which indicated the presence of dead bacteria. On the D0/C30 coating, green color was observed, indicating that viable bacteria were more prominent. The percentage of dead bacteria is shown in Figure 15c. The result revealed that D15/C15 provided a greater percentage of dead bacteria in biofilm compared to the control (p <.05, ANOVA and Tukey's HSD test).

The CLSM images of biofilm formation on coated specimens with aging are shown in Figure 16a. The surface coated by copolymers containing MPC (*i.e.*, D0/C30 and D15/C15) exhibited more dispersed and thinner biofilm compared with D30/C0 and the control. The quantitative evaluation of biofilm thickness on the coated specimens after aging is demonstrated in Figure 16b. The copolymers containing MPC (*i.e.*, D0/C30 and D15/C15) exhibited significantly thinner biofilm than D30/C0 and the control ($p < .05$, ANOVA and Tukey's HSD test). The percentage of dead bacteria was shown in Figure 16c. The result exhibited that D15/C15 increased the percentage of dead bacteria in biofilm compared to the control ($p < .05$, ANOVA and Tukey's HSD test). Among the four groups, the D15/C15 coating exhibited sparser and thinner biofilm, in addition to a greater percentage of dead bacteria, indicating that this group was the most effective in terms of its anti-biofilm effect, even after ageing.

Figure 17 presents a comparison of the thickness of biofilm between before and after immersion of the specimen in water for 28 days. No significant difference in biofilm thickness was observed between before and after immersion in all groups ($p > .05$, Student's *t*-test). Figure 18 shows the percentage of dead bacteria before and after water aging. No significant difference in the percentage of dead bacteria between before and after immersion in all groups was observed ($p > .05$, Student's *t*-test).

4.3 Discussion

An attempt to provide the restorations with antibacterial properties to inhibit plaque accumulation has been addressed in many studies. Previously, *in vitro* tests using *S. mutans* indicated that the resin composites mixed with MDPB-containing prepolymerized resin filler exhibit inhibitory effects against biofilm accumulation [9]. This antibacterial activity arises from the inhibition of bacterial growth by contact with the MDPB-containing filler [10]. In addition, it also depends on the suppression of bacterial attachment and glucan synthesis by inactivation of glucosyltransferase [9]. However, the anti-biofilm effect was attenuated by the treatment of saliva on the experimental resin composites due to the reduced contact of bacteria with MDPB by protein adsorption, although the saliva-treated polymers still exhibited bacterial adherence or growth inhibitions on their surfaces compared with control materials without MDPB. [10,13]. The protein film was considered to be a barrier in diverse cationic antibacterial surfaces; it was not only MDPB that was weakened the antibacterial and anti-biofilm effects [90–93]. The attenuation of these antibacterial effects is thought to be due to the reduction in the exposed area of the antibacterial component on the material surface.

MPC was also reported to inhibit oral biofilm formation by suppressing bacterial adherence due to its inhibition of protein adsorption; subsequently, the initial interaction between microorganisms and material surfaces was retarded [94]. This action of MPC

has been studied in various pathogens, including general and oral microbes such as *Staphylococcus aureus*, a most common pathogen, and opportunistic pathogens *Pseudomonas aeruginosa* and *Candida albicans* [27,29]. Particularly, MPC reduced the adherence of early colonizers (e.g., *Streptococcus sanguinis*) and co-aggregative bacteria (e.g., *Fusobacterium nucleatum*) in oral biofilm formation [28]. Another advantage of the MPC polymer is its excellent biocompatibility owing to its similarity with the cell-wall structure [16]. However, the compatibility of phosphorylcholine groups with cells is favorable for the viability of microorganisms [95], indicating that MPC polymer cannot inhibit the proliferation of bacteria, which was proved in experiment 3. In this study, MPC was combined with MDPB to facilitate protein repellency in the coating material. Consequently, the formation of biofilm was hindered at the initial step, which requires salivary protein adsorption prior to bacteria attachment (Figure 19) [96,97]. This effect was supported by CLSM observation, which revealed sparser biofilm formation in the copolymers containing MPC compared with those formed in D30/C0 and the control. Furthermore, MDPB exhibited bactericidal effects, and the percentage of dead bacteria was small in the group containing both MDPB and MPC. The greater percentage of viable bacteria causes tooth demineralization and enamel/dental caries because *S. mutans* can produce acids via glucose metabolism [98–101]. Thus, a smaller percentage of living bacteria is crucial to prevent oral diseases. With MPC, bacteria can be easily exposed to

MDPB due to the non-protein-coated surface and be effectively killed under an environment with plenty of saliva protein. In addition, it has been reported that MDPB exhibits a bacteriolysis effect that suppresses the bacterial growth, leading to the inhibition of extracellular-matrix synthesis to retard biofilm formation [9]. Eventually, the inhibition of biofilm formation will prevent the occurrence of secondary caries, which is caused by continual acid production beneath the biofilm [102,103]. The results obtained by CLSM and SEM revealed the synergistic properties of protein-repellent MPC and antibacterial MDPB on the surface coated with D15/C15, which caused thinner and sparser biofilm containing more dead bacteria compared with those formed in other specimens.

4.4 Summary

Due to the ability of the MPC polymer to inhibit protein adsorption, the coating composed ≥15% MPC inhibited the adsorption of protein, which is required for the initial step of biofilm formation. Additionally, ≥15% MDPB in the copolymer exhibited bactericidal effects due to its contact killing of bacteria. Both functions resulted in the dual-functional effects of protein repellency from MPC and antibacterial activity from MDPB.

GENERAL CONCLUSION

Most oral diseases are caused by bacterial infection, and it is crucial to control bacteria to maintain and promote oral health. Restorative and prosthodontic materials with antimicrobial properties are promising to prevent secondary diseases that occur in the oral cavity, which is full of bacteria. With the intention to develop useful antibacterial material like polymerizable bactericide, a novel coating material that combined synergistic functions from MDPB and MPC was developed.

Owing to the ability of MPC polymer, the coating composed of ≥15% MPC inhibited the adsorption of protein, which is required for the initial step of biofilm formation. Additionally, ≥15% MDPB in the copolymer exhibited bactericidal effects due to its contact killing of bacteria. Eventually, the copolymer composed of 15% MDPB/15% MPC effectively inhibited biofilm formation even after aging. Nevertheless, the oral environment is indeed challenging, and multiple factors need to be considered. Although hydrophobic interactions of the coating material are durable after aging, mechanical stress from mastication and cleaning should be considered.

In this study, the fabrication of a copolymer coating composed of MDPB and MPC that exhibited both protein repellency and bactericidal effects was achieved, leading to an effective anti-biofilm property. This novel, dual-functional surface coating can be applied

to a variety of dental resins for controlling bacteria in an oral environment. However, oral microbes consist of diverse microorganisms that produce more complex and harsher oral biofilm. Therefore, an assessment of the benefit of this coating for *in situ* experiments is still required to determine its potential for clinical applications in the future.

REFERENCES

[1] Imazato S, Kohno T, Tsuboi R, Thongthai P, Xu HH, Kitagawa H. Cutting-edge filler technologies to release bio-active components for restorative and preventive dentistry. Dent Mater J 2020;39:69–79

[2] Imazato S, Chen J, Ma S, Izutani N, Li F. Antibacterial resin monomers based on quaternary ammonium and their benefits in restorative dentistry. Jpn Dent Sci Rev 2012;48:115–125.

[3] Imazato S, Torii M, Tsuchitani Y, McCabe JF, Russell RRB. Incorporation of bacterial inhibitor into resin composite. J Dent Res 1994;73:1437–1443.

[4] Izutani N, Imazato S, Nakajo K, Takahashi N, Takahashi Y, Ebisu S, Russell RR. Effects of the antibacterial monomer 12-methacryloyloxydodecylpyridinium bromide (MDPB) on bacterial viability and metabolism. Eur J Oral Sci 2011;119:175–181.

[5] Imazato S, Kinomoto Y, Tarumi H, Torii M, Russell RRB, McCabe JF. Incorporation of antibacterial monomer MDPB into dentin primer. J Dent Res 1997;76:768–772.

[6] Kitagawa R, Kitagawa H, Izutani N, Hirose N, Hayashi M, Imazato S. Development of an antibacterial root canal filling system containing MDPB. J Dent Res 2014;93:1277–1282.

[7] Hirose N, Kitagawa R, Kitagawa H, Maezono H, Mine A, Hayashi M, Haapasalo M, Imazato S. Development of a cavity disinfectant containing antibacterial monomer MDPB. J Dent Res 2016;95:1487–1493.

[8] Imazato S, Ma S, Chen J, Xu HHK. Therapeutic polymers for dental adhesives: Loading resins with bio-active components. Dent Mater 2014;30:97–104.

[9] Ebi N, Imazato S, Noiri Y, Ebisu S. Inhibitory effects of resin composite containing bactericide-immobilized filler on plaque accumulation. Dent Mater 2001;17:485–491.

[10] Imazato S, Ebi N, Takahashi Y, Kaneko T, Ebisu S, Russell RR. Antibacterial activity of bactericide-immobilized filler for resin-based restoratives. Biomaterials 2003;24:3605–3609.

[11] Wahlgren M, Arnebrant T. Protein adsorption to solid surfaces. Trends Biotechnol 1991;9:201–208.

[12] Daeschel MA, McGuire J. Interrelationships between protein surface adsorption and bacterial adhesion. Biotechnol Genet Eng Rev 1998;15:413–438.

[13] Müller R, Eidt A, Hiller KA, Katzur V, Subat M, Schweikl H, Imazato S, Ruhl S, Schmalz G. Influences of protein films on antibacterial or bacteria-repellent surface coatings in a model system using silicon wafers. Biomaterials 2009;30:4921–4929.

[14] Forson AM, van der Mei HC, Sjollema J. Impact of solid surface hydrophobicity and micrococcal nuclease production on *Staphylococcus aureus* Newman biofilms. Sci Rep 2020;10:12093.

[15] Ishihara K, Ueda T, Nakabayashi N. Preparation of phospholipid polymers and their properties as polymer hydrogel membranes. Polym J 1990;22:355–360.

[16] Iwasaki Y, Ishihara K. Cell membrane-inspired phospholipid polymers for developing medical devices with excellent biointerfaces. Sci Technol Adv Mater 2012;13:064101.

[17] Ueda T, Watanabe A, Ishihara K, Nakabayashi N. Protein adsorption on biomedical polymers with a phosphorylcholine moiety adsorbed with phospholipid. J Biomater Sci Polym Ed 1992;3:185–194.

[18] Ishihara K, Nomura H, Mihara T, Kurita K, Iwasaki Y, Nakabayashi N. Why do phospholipid polymers reduce protein adsorption? J Biomed Mater Res 1998;39:323–330.

[19] Ishihara K, Fukumoto K, Iwasaki Y, Nakabayashi N. Modification of polysulfone with phospholipid polymer for improvement of the blood compatibility. Part 2. Protein adsorption and platelet adhesion. Biomaterials 1999;20:1553–1559.

[20] Lendenmann U, Grogan J, Oppenheim FG. Saliva and dental pellicle-A review. Adv Dent Res 2000;14:22–28.

[21] Hannig C, Hannig M, Attin T. Enzymes in the acquired enamel pellicle. Eur J Oral Sci 2005;113:2–13.

[22] Busscher HJ, Rinastiti M, Siswomihardjo W, van der Mei HC. Biofilm formation on dental restorative and implant materials. J Dent Res 2010;89:657–665.

[23] Engel AS, Kranz HT, Schneider M, Tietze JP, Piwowarcyk A, Kuzius T, Arnold W, Naumova EA. Biofilm formation on different dental restorative materials in the oral cavity. BMC Oral Health 2020;20:162.

[24] Goda T, Ishihara K. Soft contact lens biomaterials from bioinspired phospholipid polymers. Expert Rev Med Devices 2006;3:167–174.

[25] Yamazaki K, Kihara S, Akimoto T, Tagusari O, Kawai A, Umezu M, Tomioka J, Kormos RL, Griffith BP, Kurosawa H. EVAHEART: an implantable centrifugal blood pump for long-term circulatory support. Jpn J Thorac Cardiovasc Surg 2002;50:461–465.

[26] Kyomoto M, Moro T, Konno T, Takadama H, Yamawaki N, Kawaguchi H, Takatori Y, Nakamura K, Ishihara K. Enhanced wear resistance of modified cross-linked polyethylene by grafting with poly(2-methacryloyloxyethyl phosphorylcholine). J Biomed Mater Res A 2007;82:10–17.

[27] Hirota K, Murakami K, Nemoto K, Miyake Y. Coating of a surface with 2-methacryloyloxyethyl phosphorylcholine (MPC) co-polymer significantly reduces retention of human pathogenic microorganisms. FEMS Microbiol Lett 2005;248:37–45.

[28] Hirota K, Yumoto H, Miyamoto K, Yamamoto N, Murakami K, Hoshino Y, Matsuo T, Miyake Y. MPC-polymer reduces adherence and biofilm formation by oral bacteria. J Dent Res 2011;90:900–905.

[29] Hatsuno K, Mukohyama H, Horiuchi S, Iwasaki Y, Yamamoto N, Akiyoshi K, Taniguchi H. Poly (MPC-co-BMA) coating reduces the adhesion of *Candida albicans* to poly (methyl methacrylate) surfaces. Prosthodont Res Pract 2006;5:21–25.

[30] Nishigochi S, Ishigami T, Maruyama T, Hao Y, Ohmukai Y, Iwasaki Y, Matsuyama H. Improvement of antifouling properties of polyvinylidene fluoride hollow fiber membranes by simple dip coating of phosphorylcholine copolymer *via* hydrophobic interactions. Ind Eng Chem Res 2014;53:2491–2497.

[31] Ishihara K, Mu M, Konno T. Water-soluble and amphiphilic phospholipid copolymers having 2-methacryloyloxyethyl phosphorylcholine units for the solubilization of bioactive compounds. J. Biomater Sci Polym Ed 2018;29:844–862.

[32] Imazato S, Russell RRB, McCabe JF. Antibacterial activity of MDPB polymer incorporated in dental resin. J Dent 1995;23:177–181.

[33] Goda T, Goto Y, Ishihara K. Cell-penetrating macromolecules: Direct penetration of amphipathic phospholipid polymers across plasma membrane of living cells. Biomaterials 2010;31:2380–2387.

[34] Imazato S. Bio-active restorative materials with antibacterial effects: new dimension of innovation in restorative dentistry. Dent Mater J 2009;28:11–19.

[35] Zhang N, Weir MD, Romberg E, Bai Y, Xu HHK. Development of novel dental adhesive with double benefits of protein-repellent and antibacterial capabilities. Dent Mater 2015;31:845–854.

[36] Zhang N, Melo MA, Chen C, Liu J, Weir MD, Bai Y, Xu HH. Development of a multifunctional adhesive system for prevention of root caries and secondary caries. Dent Mater 2015;31:1119–1131.

[37] Zhang N, Ma J, Melo MAS, Weir MD, Bai Y, Xu HHK. Protein-repellent and antibacterial dental composite to inhibit biofilms and caries. J Dent 2015;43:225–234.

[38] Zhang N, Melo MAS, Antonucci JM, Lin NJ, Lin-Gibson S, Bai Y, Xu HHK. Novel Dental Cement to Combat Biofilms and Reduce Acids for Orthodontic Applications to Avoid Enamel Demineralization. Materials 2016;9:413.

[39] Zhang N, Zhang K, Melo MA, Weir MD, Xu DJ, Bai Y, Xu HH. Effects of Long-Term Water-Aging on Novel Anti-Biofilm and Protein-Repellent Dental Composite. Int J Mol Sci 2017;18:186.

[40] Zhang N, Zhang K, Weir MD, Xu DJ, Reynolds MA, Bai Y, Xu HHK. Effects of water-aging for 6 months on the durability of a novel antimicrobial and protein-repellent dental bonding agent. Int J Oral Sci 2018;10:18.

[41] Zhang N, Zhang K, Xie X, Dai Z, Zhao Z, Imazato S, Al-Dulaijan YA, Al-Qarni FD, Weir MD, Reynolds MA, Bai Y, Wang L, Xu HHK. Nanostructured Polymeric Materials with Protein-Repellent and Anti-Caries Properties for dental applications. Nanomaterials 2018;8:393.

[42] Takahashi N, Iwasa F, Inoue Y, Morisaki H, Ishihara K, Baba K. Evaluation of the durability and antiadhesive action of 2-methacryloyloxyethyl phosphorylcholine grafting on an acrylic resin denture base material. J Prosthet Dent 2014;112:194–203.

[43] Ferreira P, Alves P, Coimbra P, Gil MH. Improving polymeric surfaces for biomedical applications: a review. J Coat Technol Res 2015;12:463–475.

[44] Ohshio M, Ishihara K, Yusa S. Self-association behavior of cell membrane-inspired amphiphilic random copolymers in water. Polymers 2019;11:327.

[45] Shiu HT, Goss B, Lutton C, Crawford R, Xiao Y. Controlling whole blood activation and resultant clot properties by carboxyl and alkyl functional groups on material surfaces: a possible therapeutic approach for enhancing bone healing. J Mater Chem B 2014;2:3009–3021.

[46] Kiaei D, Hoffman AS, Horbett TA. Radio-frequency gas discharge (RFGD) fluorination of polymers: Protein and cell interactions at RFGD-fluorinated interfaces. Radiat Phys Chem 1995;46:191–197.

[47] Wilson CJ, Clegg RE, Leavesley DI, Pearcy MJ. Mediation of biomaterial–cell interactions by adsorbed proteins: A review. Tissue Eng 2005;11:1–18.

[48] Wei Q, Becherer T, Angioletti-Uberti S, Dzubiella J, Wischke C, Neffe AT, Lendlein A, Ballauff M, Haag R. Protein interactions with polymer coatings and biomaterials. Angew Chem Int Ed 2014;53:8004–8031.

[49] Rahmati M, Mozafari M. Protein adsorption on polymers. Mater Today Commun 2018;17:527–540.

[50] Rabe M, Verdes D, Seeger S. Understanding protein adsorption phenomena at solid surfaces. Adv Colloid Interface Sci 2011;162:87–106.

[51] Ishihara K, Ziats NP, Tierney BP, Nakabayashi N, Anderson JM. Protein adsorption from human plasma is reduced on phospholipid polymers. J Biomed Mater Res 1991;25:1397–1407.

[52] Ishihara K, Oshida H, Endo Y, Ueda T, Watanabe A, Nakabayashi N. Hemocompatibility of human whole blood on polymers with a phospholipid polar group and its mechanism. J Biomed Mater Res 1992;26:1543–1552.

.

[53] Corkhill PH, Jolly AM, Ng CO, Tighe BJ. Synthetic hydrogels: 1. Hydroxyalkyl acrylate and methacrylate copolymers - water binding studies. Polymer 1987;28:1758–1766.

[54] Lu DR, Lee SJ, Park K. Calculation of solvation interaction energies for protein adsorption on polymer surfaces. J Biomater Sci Polym Ed 1992;3:127–147.

[55] Ballet T, Boulange L, Brechet Y, Bruckert F, Weidenhaupt M. Protein conformational changes induced by adsorption onto material surfaces: an important issue for biomedical applications of material science. Bull Pol Acad Sci-Tech Sci 2010;58:303–315.

[56] Moskovitz Y, Srebnik S. Conformational changes of globular proteins upon adsorption on a hydrophobic surface. Phys Chem Chem Phys 2014;16:11698–11707.

[57] Schramm FD, Schroeder K, Jonas K. Protein aggregation in bacteria. FEMS Microbiol Rev 2019;44:54–72.

[58] Ishihara K, Iwasaki Y. Reduced protein adsorption on novel phospholipid polymers. J Biomater Appl 1998;13:111–127.

[59] Ishihara K, Takai M. Bioinspired interface for nanobiodevices based on phospholipid polymer chemistry. J R Soc Interface 2009;6(Suppl 3):S279–291.

[60] Goda T, Ishihara K, Miyahara Y. Critical update on 2-methacryloyloxyethyl phosphorylcholine (MPC) polymer science. J Appl Polym Sci 2015;132:41766.

[61] Ishihara K. Successful development of biocompatible polymers designed by natures original inspiration. Procedia Chem 2012;4:34–38.

[62] Yamasaki A, Imamura Y, Kurita K, Iwasaki Y, Nakabayashi N, Ishihara K. Surface mobility of polymers having phosphorylcholine groups connected with various bridging units and their protein adsorption-resistance properties. Colloids Surf B 2003;28:53–62.

[63] Ueda H, Watanabe J, Konno T, Takai M, Saito A, Ishihara K. Asymmetrically functional surface properties on biocompatible phospholipid polymer membrane for bioartificial kidney. J Biomed Mater Res A 2006;77:19–27.

[64] Soletti L, Nieponice A, Hong Y, Ye SH, Stankus JJ, Wagner WR, Vorp DA. *In vivo* performance of a phospholipid-coated bioerodable elastomeric graft for small-diameter vascular applications. J Biomed Mater Res A 2011;96:436–448.

[65] Lewis AL, Furze JD, Small S, Robertson JD, Higgins BJ, Taylor S, Ricci DR. Long-term stability of a coronary stent coating post-implantation. J Biomed Mater Res 2002;63:699–705.

[66] Iwasaki Y, Uchiyama S, Kurita K, Morimoto N, Nakabayashi N. A nonthrombogenic gas-permeable membrane composed of a phospholipid polymer skin film adhered to a polyethylene porous membrane. Biomaterials 2002;23:3421–3427.

[67] Jenzano JW, Hogan SL, Noyes CM, Featherstone GL, Lundblad RL. Comparison of five techniques for the determination of protein content in mixed human saliva. Anal Biochem 1986;159:370–376.

[68] Barreto MSC, Elzinga EJ, Alleoni LRF. The molecular insights into protein adsorption on hematite surface disclosed by in-situ ATR-FTIR/2D-COS study. Sci Rep 2020;10:13441.

[69] Lee E, Kim I, Nam H, Jeon H, Lim G. Modulation of saliva pattern and accurate detection of ovulation using an electrolyte pre-deposition-based method: a pilot study. Analyst 2020;145:1716–1723.

[70] Lewis AL. Phosphorylcholine-based polymers and their use in the prevention of biofouling. Colloids Surf B 2000;18:261–275.

[71] Lamy E, Simões C, Carreira L, Capela e Silva F. Saliva protein composition relates with interindividual variations in bread sensory ratings. Starch 2021;73:2000052.

[72] Yan W, Apweiler R, Balgley BM, Boontheung P, Bundy JL, Cargile BJ, Cole S, Fang X, Gonzalez-Begne M, Griffin TJ, Hagen F, Hu S, Wolinsky LE, Lee CS, Malamud D, Melvin JE, Menon R, Mueller M, Qiao R, Rhodus NL, Sevinsky JR, States D, Stephenson JL, Than S, Yates JR, Yu W, Xie H, Xie Y, Omenn GS, Loo JA, Wong DT. Systematic comparison of the human saliva and plasma proteomes. Proteomics Clin Appl 2009;3:116-134.

[73] Bandhakavi S, Stone MD, Onsongo G, Van Riper SK, Griffin TJ. A dynamic range compression and three-dimensional peptide fractionation analysis platform expands proteome coverage and the diagnostic potential of whole saliva. J Proteome Res 2009;8:5590-5600.

[74] Xiao X, Liu Y, Guo Z, Liu X, Sun H, Li Q, Sun W. Comparative proteomic analysis of the influence of gender and acid stimulation on normal human saliva using LC/MS/MS. Proteomics Clin Appl 2017;11:1600142.

[75] Sarkar A, Xu F, Lee S. Human saliva and model saliva at bulk to adsorbed phases – similarities and differences. Adv Colloid Interface Sci 2019;273:102034.

[76] Kun R, Szekeres M, Dékány I. Isothermal titration calorimetric studies of the pH induced conformational changes of bovine serum albumin. J Therm Anal Calorim 2009;96(3):1009-1017.

[77] Van Oss CJ, Wu W, Giese RF, Naim JO. Interaction between proteins and inorganic oxides-Adsorption of albumin and its desorption with a complexing agent. Colloids Surf B 1995;4(3):18518-9.

[78] Namba N, Yoshida Y, Nagaoka N, Takashima S, Matsuura-Yoshimoto K, Maeda H, Van Meerbeek B, Suzuki K, Takashiba S. Antibacterial effect of bactericide immobilized in resin matrix. Dent Mater 2009;25:424–430.

[79] Denyer SP. Mechanisms of action of antibacterial biocides. Int Biodeterior Biodegradation 1995;36:227–245.

[80] Vieira DB. Cationic lipids and surfactants as antifungal agents: mode of action. J Antimicrob Chemother 2006;58:760–767.

[81] Gerba CP. Quaternary ammonium biocides: Efficacy in application. Appl Environ Microbiol 2015;81:464–469.

[82] Alkhalifa S, Jennings MC, Granata D, Klein M, Wuest WM, Minbiole KPC, Carnevale V. Analysis of the destabilization of bacterial membranes by quaternary ammonium compounds: A combined experimental and computational study. ChemBioChem 2020;21:1510–1516.

[83] Imazato S, Ebi N, Tarumi H, Russell RR, Kaneko T, Ebisu S. Bactericidal activity and cytotoxicity of antibacterial monomer MDPB. Biomaterials 1999;20:899–903.

[84] Yoshikawa K, Clark DT, Brailsford SR, Beighton D, Watson TF, Imazato S, Momoi Y. The Effect of antibacterial monomer MDPB on the growth of organisms associated with root caries. Dent Mater J 2007;26:388–392.

[85] Izutani N, Imazato S, Noiri Y, Ebisu S. Antibacterial effects of MDPB against anaerobes associated with endodontic infections: Antimicrobial effects of MDPB. Int Endod J 2010;43:637–645.

[86] Imazato S, Torii Y, Takatsuka T, Inoue K, Ebi N, Ebisu S. Bactericidal effect of dentin primer containing antibacterial monomer methacryloyloxydodecylpyridinium bromide (MDPB) against bacteria in human carious dentin. J Oral Rehabil 2001;28:314–319.

[87] Hashimoto M, Hirose N, Kitagawa H, Yamaguchi S, Imazato S. Improving the durability of resin-dentin bonds with an antibacterial monomer MDPB. Dent Mater J 2018;37:620–627.

[88] Imazato S, Ehara A, Torii M, Ebisu S. Antibacterial activity of dentine primer containing MDPB after curing. J Dent 1998;26:267–271.

[89] Imazato S, Kinomoto Y, Tarumi H, Ebisu S, Tay FR. Antibacterial activity and bonding characteristics of an adhesive resin containing antibacterial monomer MDPB. Dent Mater 2003;19:313–319.

[90] Cen L, Neoh KG, Kang ET. Surface functionalization technique for conferring antibacterial properties to polymeric and cellulosic surfaces. Langmuir 2003;19:10295–10303.

[91] Kügler R, Bouloussa O, Rondelez F. Evidence of a charge-density threshold for optimum efficiency of biocidal cationic surfaces. Microbiology 2005;151:1341–1348.

[92] Murata H, Koepsel RR, Matyjaszewski K, Russell AJ. Permanent, non-leaching antibacterial surfaces–2: How high density cationic surfaces kill bacterial cells. Biomaterials 2007;28:4870–4879.

[93] Li F, Weir MD, Fouad AF, Xu HHK. Effect of salivary pellicle on antibacterial activity of novel antibacterial dental adhesives using a dental plaque microcosm biofilm model. Dent Mater 2014;30:182–191.

[94] Fujiwara N, Yumoto H, Miyamoto K, Hirota K, Nakae H, Tanaka S, Murakami K, Kudo Y, Ozaki K, Miyake Y. 2-Methacryloyloxyethyl phosphorylcholine (MPC)-polymer suppresses an increase of oral bacteria: a single-blind, crossover clinical trial. Clin Oral Invest 2019;23:739–746.

[95] Noree S, Thongthai P, Kitagawa H, Imazato S, Iwasaki Y. Reduction of acidic erosion and oral bacterial adhesion through the immobilization of zwitterionic polyphosphoesters on mineral substrates. Chem Lett 2019;48:1529–1532.

[96] Huang R, Li M, Gregory RL. Bacterial interactions in dental biofilm. Virulence 2011;2:435–444.

[97] Wolff MS, Larson C. The cariogenic dental biofilm: good, bad or just something to control? Braz Oral Res 2009;23:31–38.

[98] Paradella TC, Koga-Ito CY, Jorge AOC. Ability of different restorative materials to prevent *in situ* secondary caries: analysis by polarized light-microscopy and energy-dispersive X-ray. Eur J Oral Sci 2008;116:375–380.

[99] Asención Diez MD, Demonte AM, Guerrero SA, Ballicora MA, Iglesias AA. The ADP-glucose pyrophosphorylase from *Streptococcus mutans* provides evidence for the regulation of polysaccharide biosynthesis in Firmicutes: ADP-Glc PPases in Firmicutes. Mol Microbiol 2013;90:1011–1027.

[100] Kim K, An J-S, Lim B-S, Ahn S-J. Effect of bisphenol A glycol methacrylate on virulent properties of *Streptococcus mutans* UA159. Caries Res 2019;53:84–95.

[101] Kitagawa H, Miki-Oka S, Mayanagi G, Abiko Y, Takahashi N, Imazato S. Inhibitory effect of resin composite containing S-PRG filler on *Streptococcus mutans* glucose metabolism. J Dent 2018;70:92–96.

[102] Hayati F, Okada A, Kitasako Y, Tagami J, Matin K. An artificial biofilm induced secondary caries model for *in vitro* studies: Biofilm induced secondary caries model. Aust Dent J 2011;56:40–47.

[103] Lima FG, Romano AR, Correa MB, Demarco FF. Influence of microleakage, surface roughness and biofilm control on secondary caries formation around composite resin restorations: an *in situ* evaluation. J Appl Oral Sci 2009;17:61–65.

TABLE LEGEND

TABLE 1. Experimentally synthesized copolymers.

FIGURE LEGENDS

Figure 1. Chemical structures of monomer.

a:12-methacryloyloxydodecylpyridinium bromide (MDPB)

b: 2-methacryloyloxyethyl phosphorylcholine (MPC)

c: n-butyl methacrylate (BMA)

Figure 2. MPC polymer and its characteristics.

a: Structure inspired by a cell membrane-like construction.

b: Superhydrophillic property of MPC.

Figure 3. Procedure of copolymer synthesis.

Figure 4. Copolymer and coating solution used

a: Copolymer powder (D15/C15)

b: Coating solution

Figure 5. Fluorescence microscopy images with fluorescence intensity.

a: PMMA surface coated with FITC-labeled copolymers.

b: Resin composites surface-coated with FITC-labeled copolymers.

(i) Bare resin (control), (ii) f-D0/C30, (iii) f-D5/C25, (iv) f-D15/C15, (v) f-D25/C5, and (vi) f-D30/C0.

The magnification of the fluorescence microscope is 10×.

Figure 6. Contact angles of each coating surface.

a: Advancing contact angles.

b: Receding contact angles.

The error bar represents the standard deviation. A, B, C, D, E: No significant difference between the bars indicated with identical letters (ANOVA, Tukey's HSD test, $p > .05$, n = 5).

Figure 7. Scheme of coating on dental resins *via* hydrophobic interactions.

(i) Bare dental resins, (ii) D0/C30, (iii) D15/C15, and (iv) D30/C0.

Figure 8. Protein adsorption test procedure.

a: Quantitative test of BSA or filtered human saliva.

b: Visualization of adsorption of FITC-BSA adsorption.

Figure 9. Protein adsorption on the surfaces after 2-hour immersion in protein solution.

a: Amount of adsorbed BSA.

b: Fluorescence microscopy images of adsorbed FITC-conjugated BSA.

c: Amount of adsorbed salivary protein.

The error bar represents the standard deviation. (i) Control, (ii) D0/C30, (iii) D15/C15, and (iv) D30/C0. A, B, C: No significant difference between the bars indicated with identical letters (ANOVA, Tukey's HSD test, $p > .05$, n = 5).

Figure 10. Scheme of protein adsorption.

a: Protein adsorption on hydrophobic surface.

b: Protein adsorption on MPC-coated surface.

Figure 11. Procedure of on-disc culture assay.

Figure 12. Number of *S. mutans* after incubation on copolymer-coated disc with well for 24 h.

a: Before 28-day immersion in water.

b: After 28-day immersion in water.

c: Comparison between before and after 28-day immersion in water.

Hatched bar represents the number of *S.mutans* on the coated disc after immersion. The error bar represents the standard deviation. Asterisks represent statistically significant

difference from control (ANOVA, Tukey's HSD test, $p < .05$, n = 5). 'n.s.' denotes no significant difference between two groups. (Student's *t*-test, $p > .05$, n=5).

Figure 13. Procedure of biofilm formation test.

Figure 14. SEM images of *S. mutans* biofilm formed after 48-hour incubation on the surface of coated specimen.

i) Control, ii) D0/C30, iii) D15/C15, and (iv) D30/C0.

Figure 15. *S. mutans* biofilm formation after 48-hour incubation on the surface of coated specimen.

a: CLSM images i) Control, ii) D0/C30, iii) D15/C15, and iv) D30/C0.

b: Thickness of biofilm analyzed from CLSM images. Asterisks represent statistically significant difference from control (ANOVA, Tukey's HSD test, $p < .05$, n = 5).

c: Percentage of dead bacteria analyzed from CLSM images. Hashtag represents statistically significant increase from control (ANOVA, Tukey's HSD test, $p < .05$, n = 3).

Figure 16. *S. mutans* biofilm formation after 48-hour incubation on the surface of coated specimen with ageing.

a: CLSM images i) Control, ii) D0/C30, iii) D15/C15, and iv) D30/C0.

b: Thickness of biofilm analyzed from CLSM images. Asterisks represent statistically significant difference from control (ANOVA, Tukey's HSD test, $p < .05$, n = 5).

c: Percentage of dead bacteria analyzed from CLSM images. Hashtag represents statistically significant increase from control (ANOVA, Tukey's HSD test, $p < .05$, n = 3).

Figure 17. Comparison of the thickness of biofilm analyzed from CLSM images before and after 28-day immersion of the specimen.

The error bar represents the standard deviation. Hatched bars with black border represent the data after 28-day immersion. 'n.s.' denotes no significant difference between two groups. (Student's *t*-test, $p > .05$, n = 5).

Figure 18. Comparison of the percentage of dead bacteria analyzed from CLSM images before and after 28-day immersion of the specimen.

Plain bars represent dead bacteria. Hatched bars represent the data after 28-day immersion. 'n.s.' denotes no significant difference between two groups. (Student's t-test, $p > .05$, n = 3).

Figure 19. Scheme of dual functions of protein repellency and antibacterial effect.

(i) Dental resins with immobilized MDPB exhibit antibacterial effects, which depend on the contact inhibition of bacteria. (ii) However, their effectiveness can be readily reduced by coverage with salivary protein. (iii) The novel surface coating composed of MDPB and MPC exhibits protein repellency and bactericidal effect.

Table 1. Experimentally synthesized copolymers.

	Composition (mol%)		
	MDPB	MPC	BMA
D0 / C30	0	30	70
D5 / C25	5	25	70
D15 / C15	15	15	70
D25 / C5	25	5	70
D30 / C0	30	0	70

a

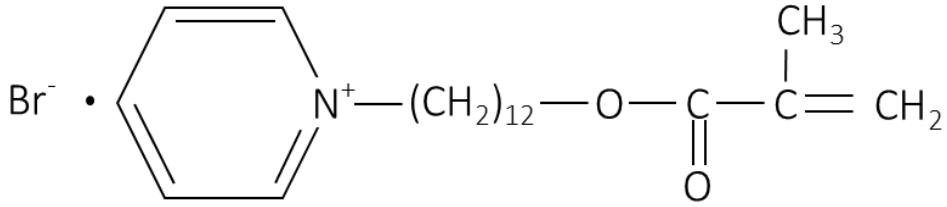

b

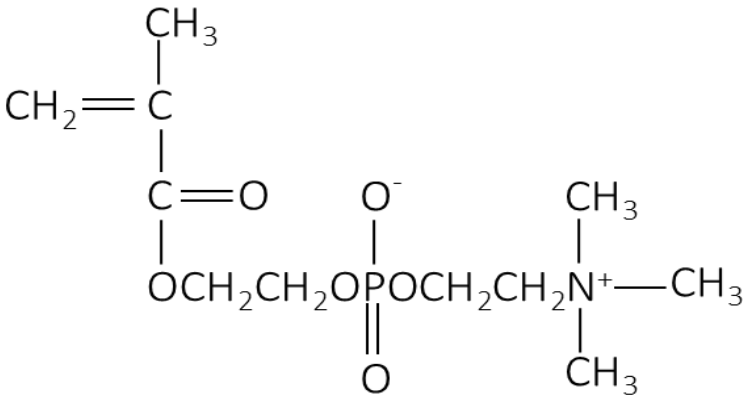

c

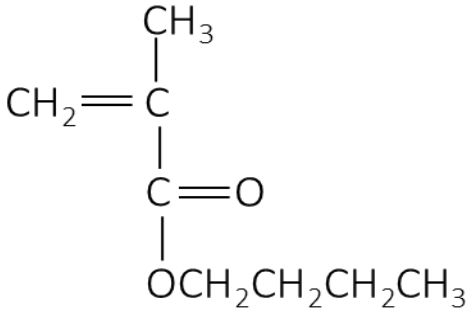

Figure 1. Chemical structures of monomer.
a:12-methacryloyloxydodecylpyridinium bromide (MDPB)
b: 2-methacryloyloxyethyl phosphorylcholine (MPC)
c: n-butyl methacrylate (BMA)

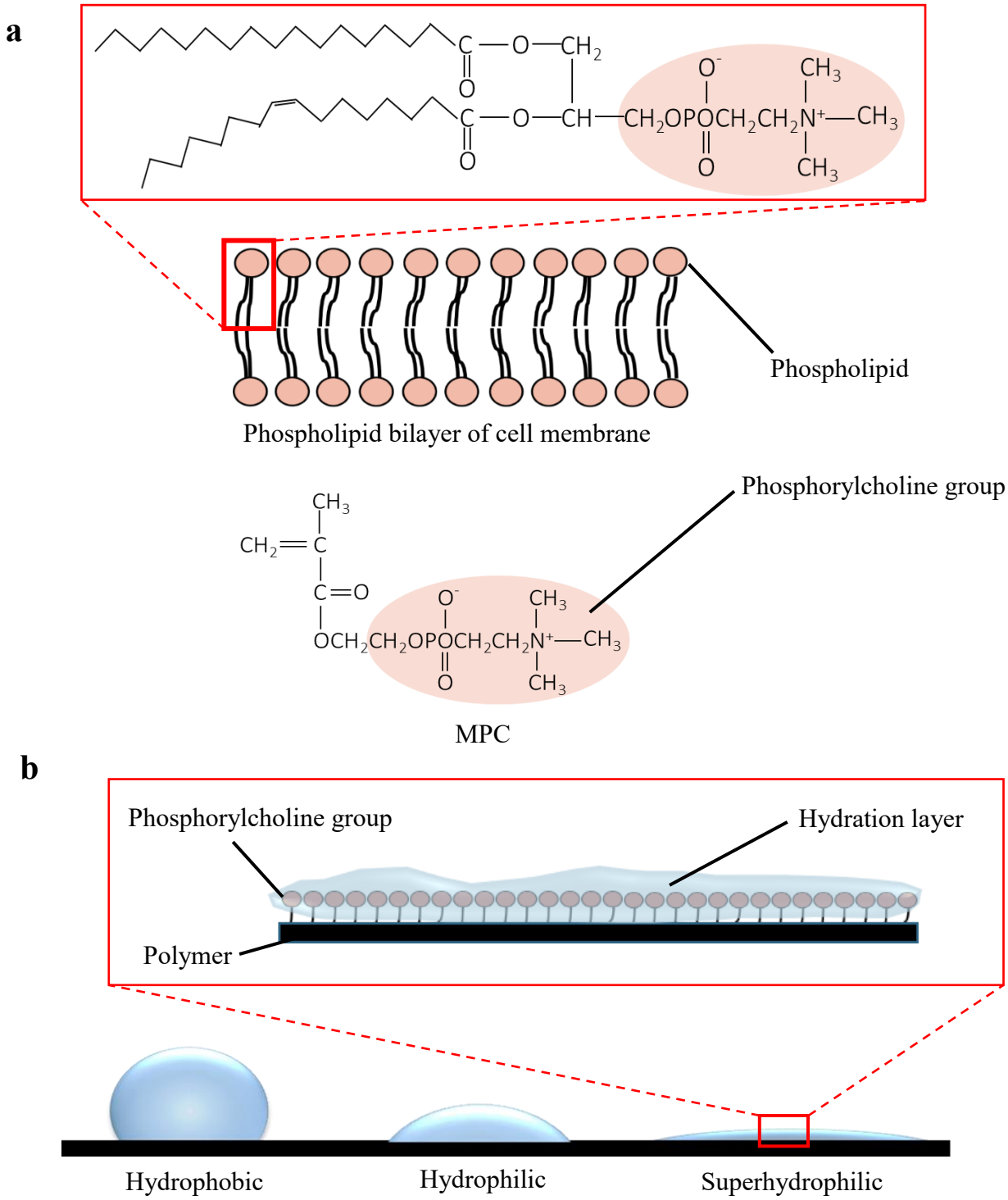

Figure 2. MPC polymer and its characteristics.
a: Structure inspired by a cell membrane-like construction.
b: Superhydrophillic property of MPC.

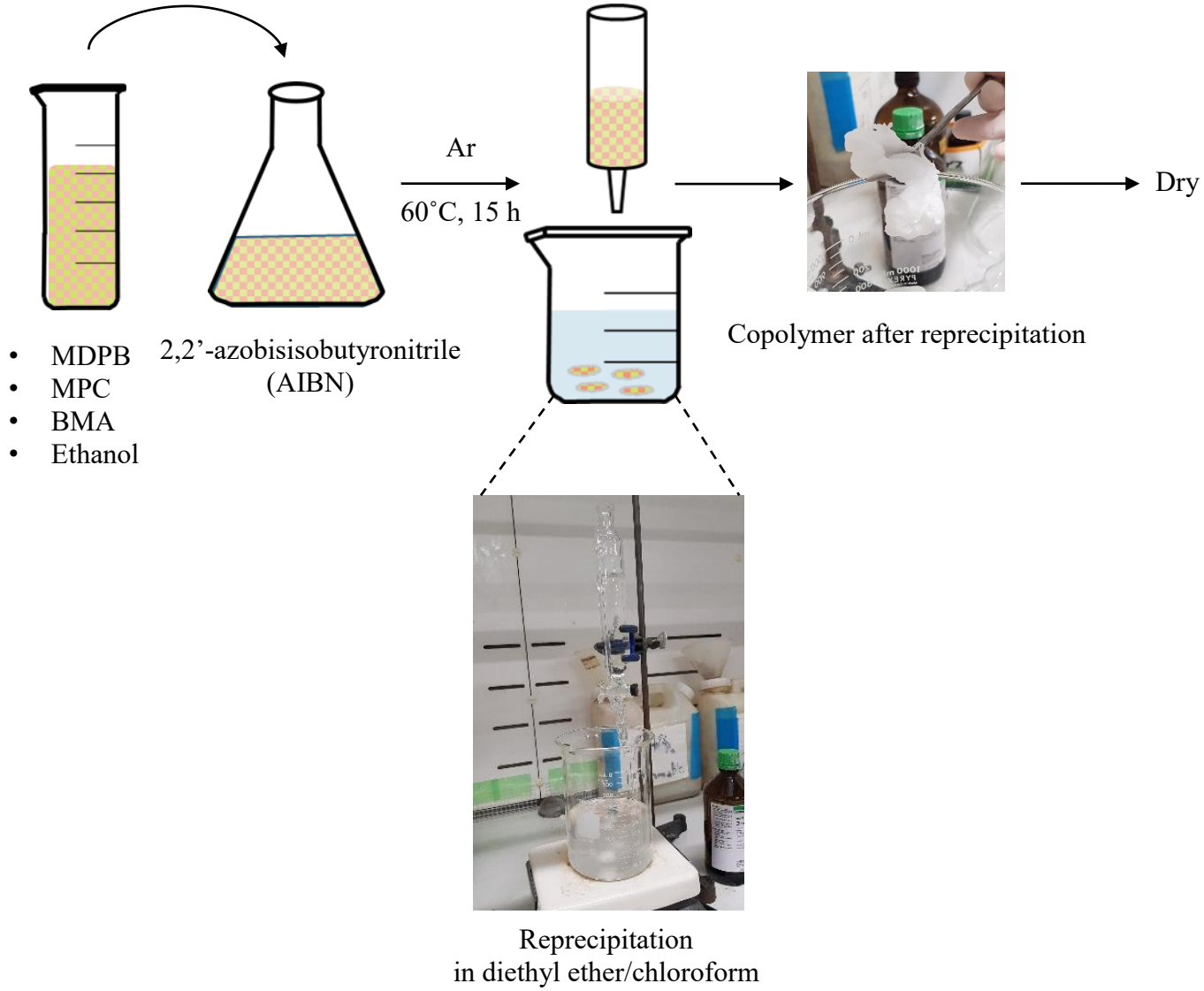

Figure 3. Procedure of copolymer synthesis.

a

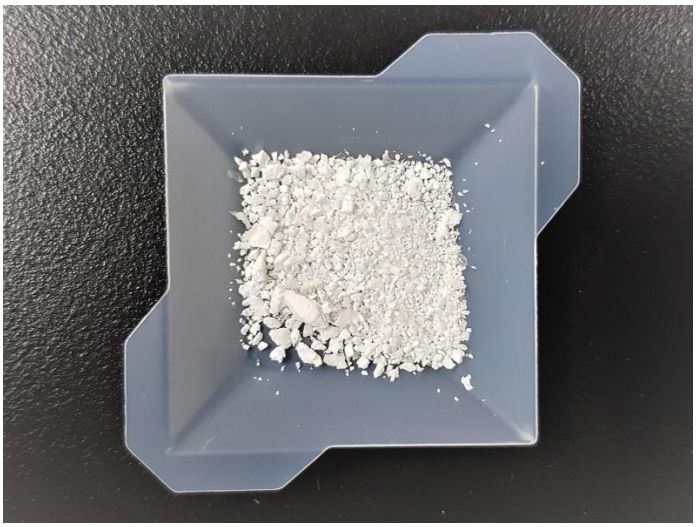

b

Figure 4. Copolymer and coating solution used.
a: Copolymer powder (D15/C15)
b: Coating solution

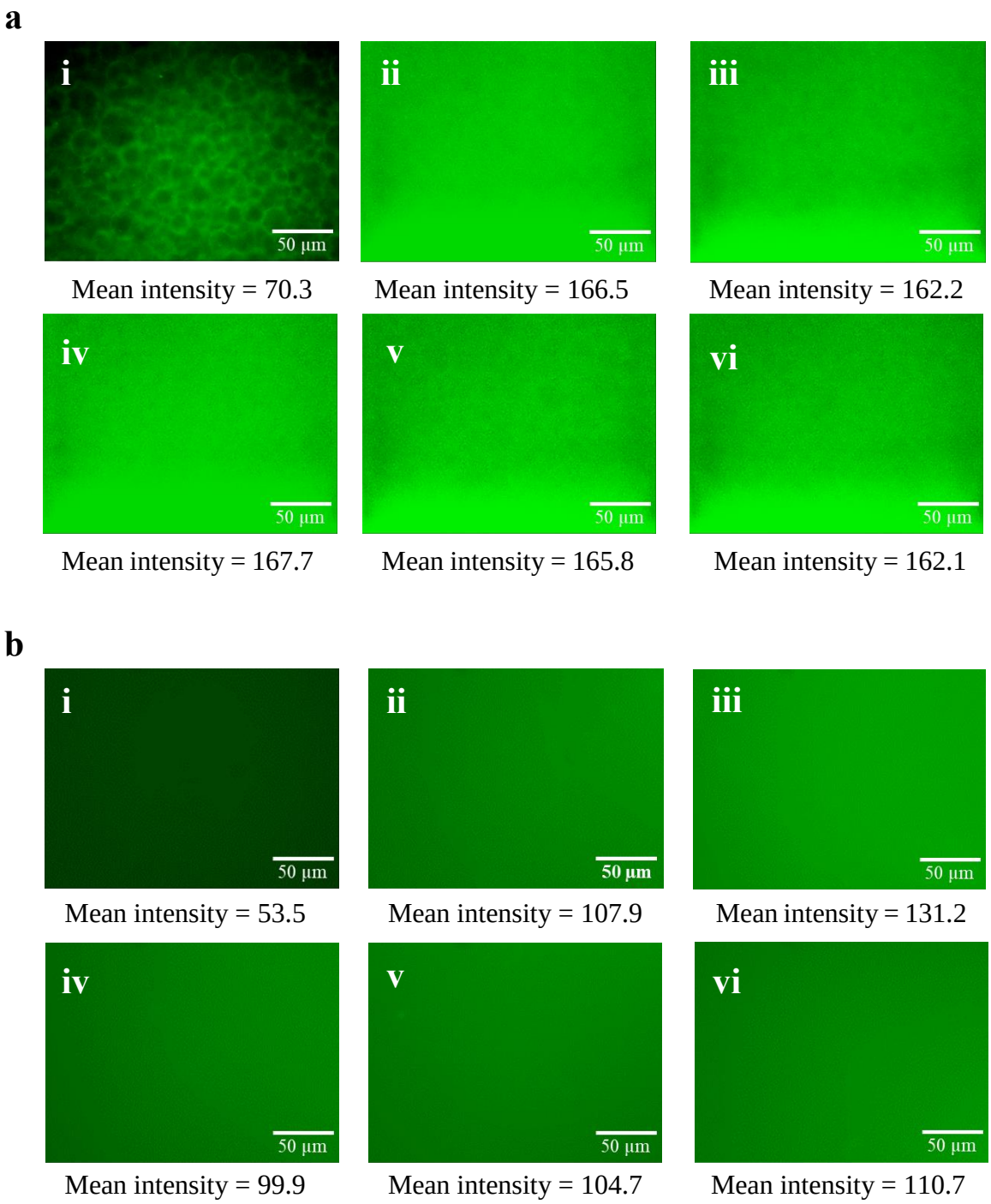

Figure 5. Fluorescence microscopy images with fluorescence intensity.
a: PMMA surface coated with FITC-labeled copolymers.
b: Resin composites surface-coated with FITC-labeled copolymers.
(i) Bare resin (control), (ii) f-D0/C30, (iii) f-D5/C25, (iv) f-D15/C15, (v) f-D25/C5, and (vi) f-D30/C0.
The magnification of the fluorescence microscope is 10×.

a

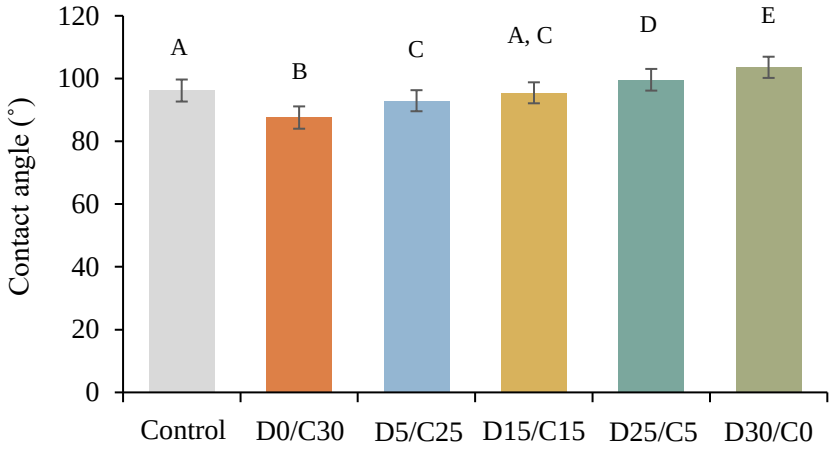

b

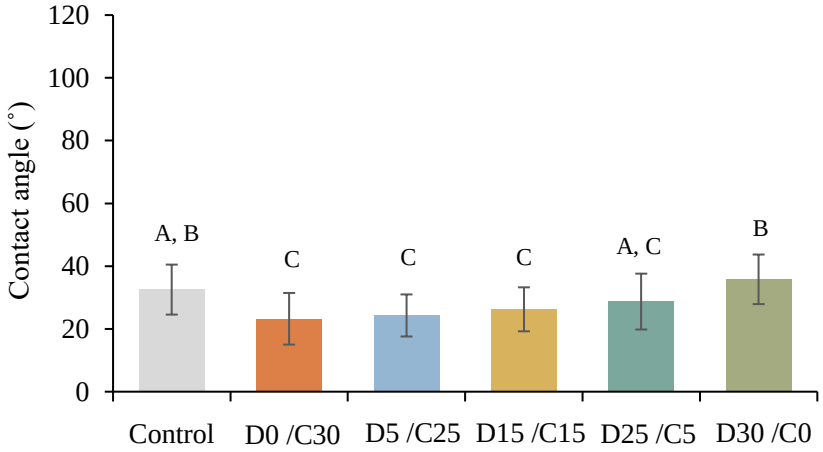

Figure 6. Contact angles of each coating surface.
a: Advancing contact angles.
b: Receding contact angles.
The error bar represents the standard deviation. A, B, C, D, E: No significant difference between the bars indicated with identical letters (ANOVA, Tukey's HSD test, $p > .05$, n = 5).

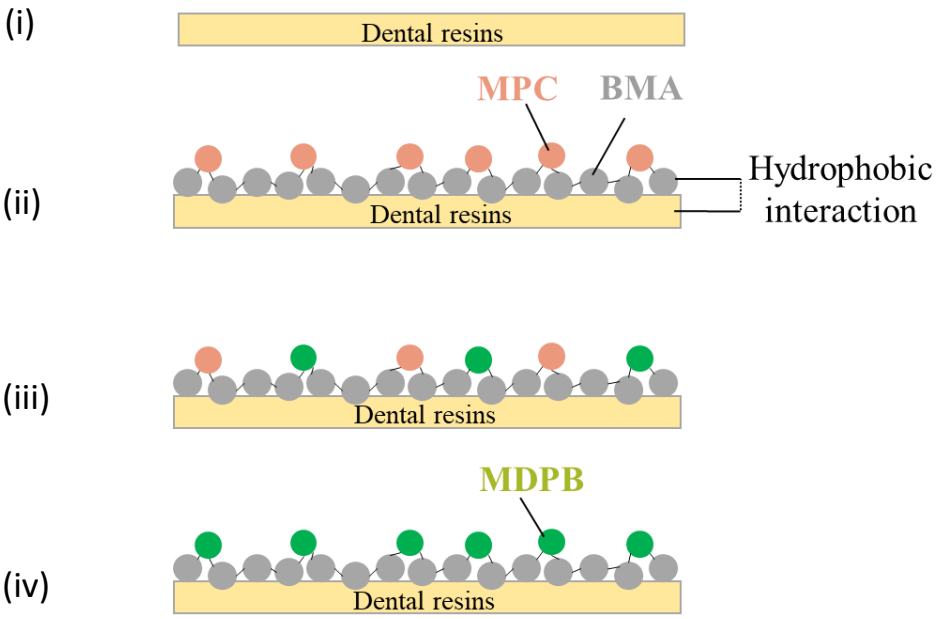

Figure 7. Scheme of coating on dental resins *via* hydrophobic interactions.
(i) Bare dental resins, (ii) D0/C30, (iii) DC15/C15, and (iv) D30/C0.

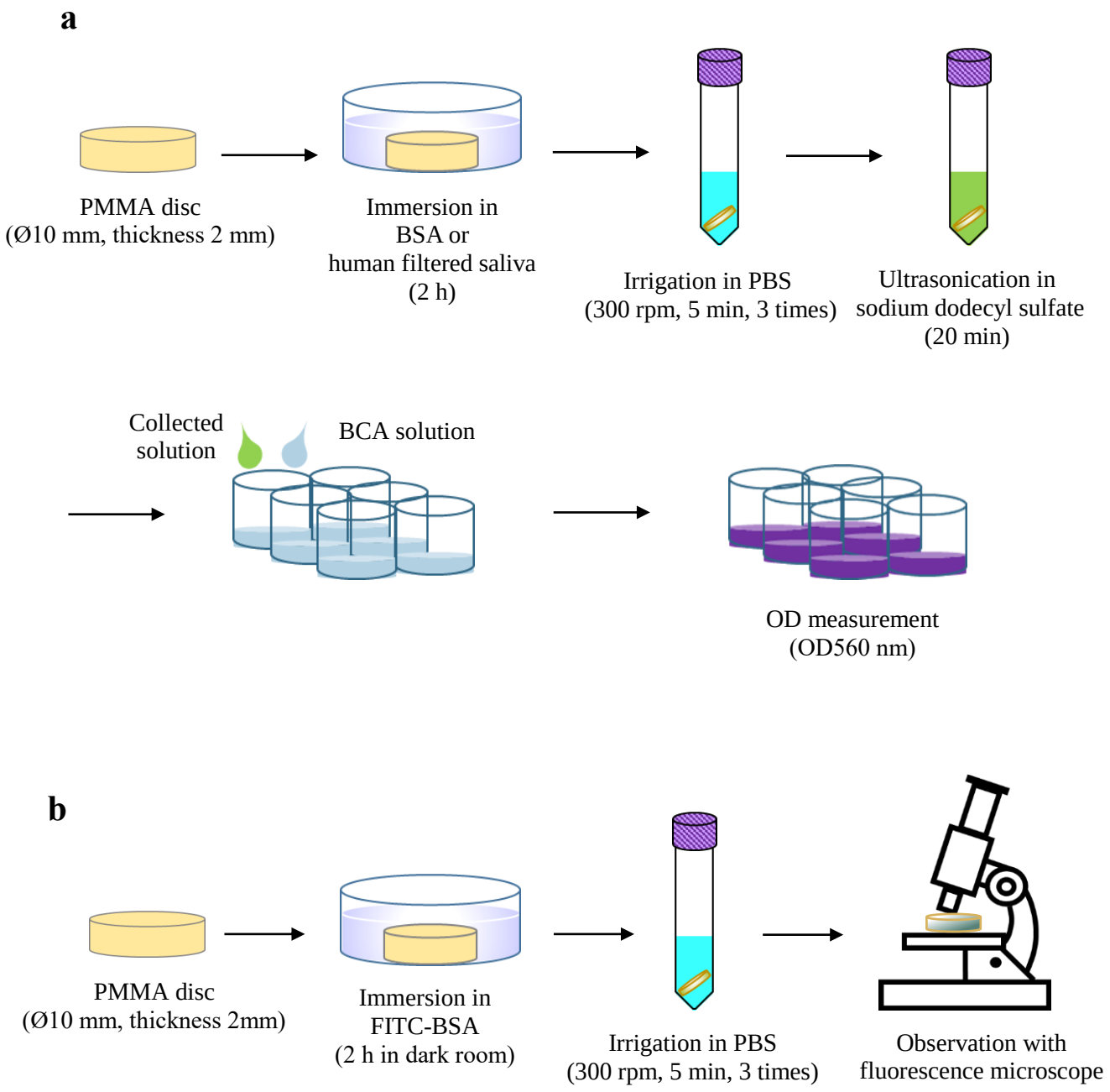

Figure 8. Procedure of protein adsorption test.
a: Quantitative test of BSA or filtered human saliva.
b: Visualization of adsorption of FITC-BSA adsorption.

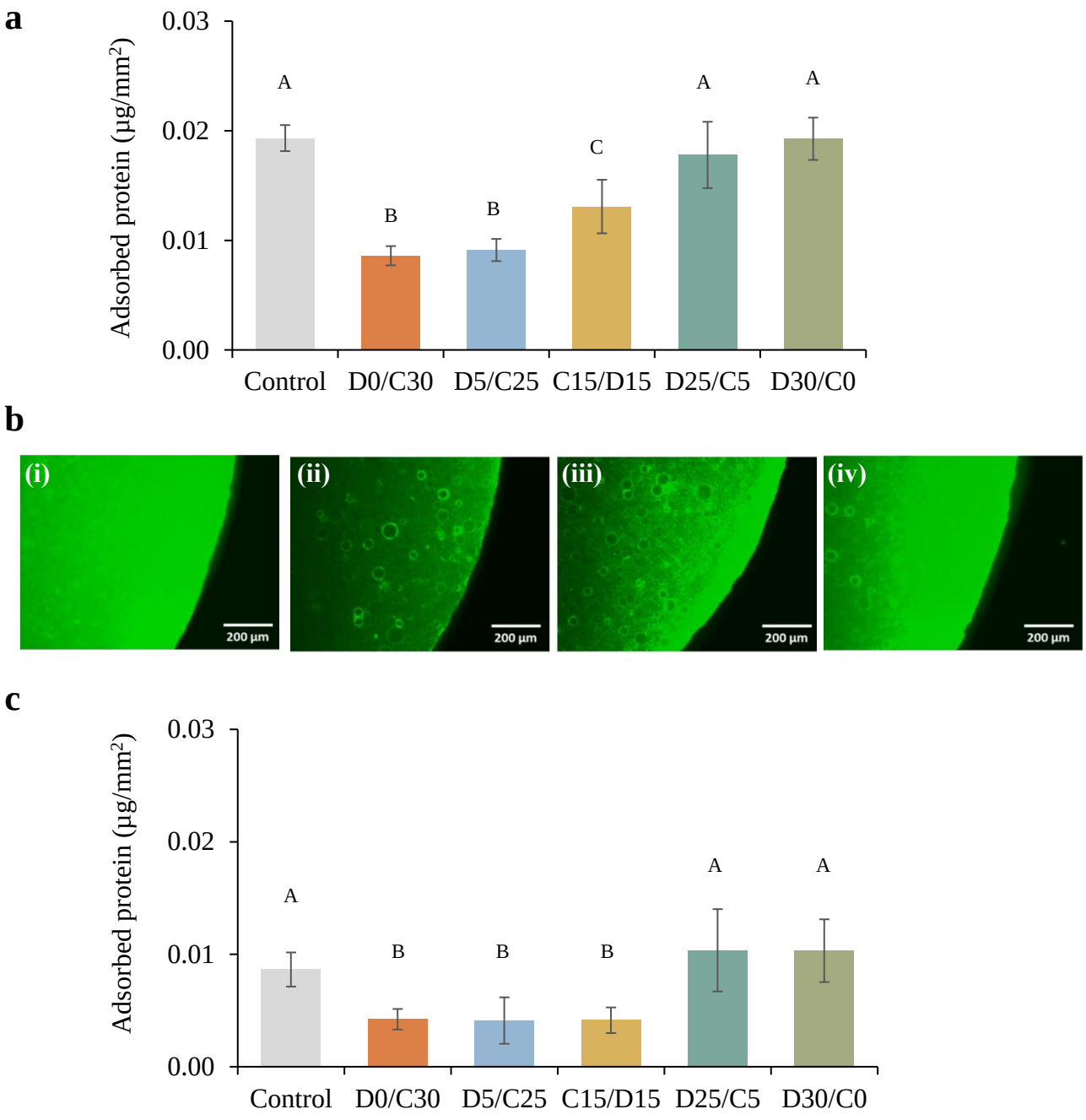

Figure 9. Protein adsorption on the surfaces after 2-hour immersion in protein solution.

a: Amount of adsorbed BSA.

b: Fluorescence microscopy images of adsorbed FITC-conjugated BSA.

c: Amount of adsorbed salivary protein.

The error bar represents the standard deviation. (i) Control, (ii) D0/C30, (iii) D15/C15, and (iv) D30/C0. A, B, C: No significant difference between the bars indicated with identical letters (ANOVA, Tukey's HSD test, $p > .05$, n = 5).

a

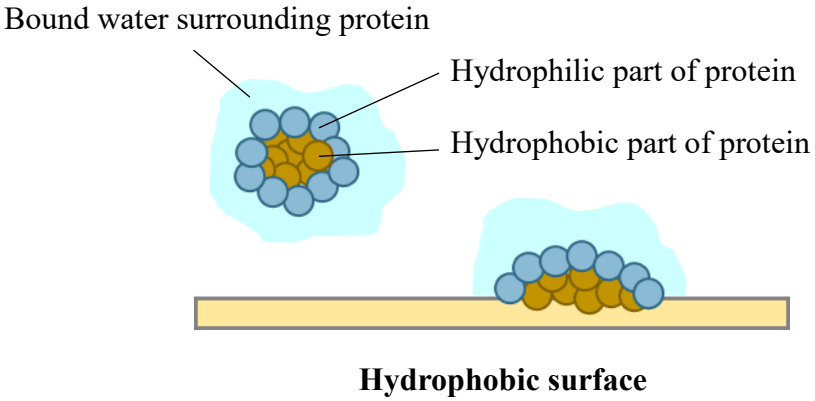

b

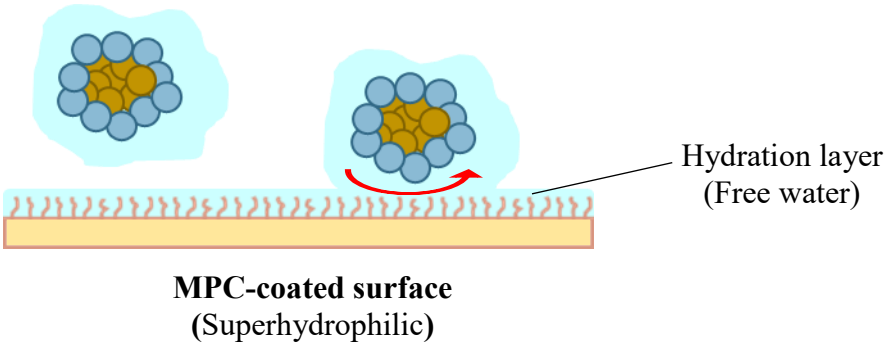

Figure 10. Scheme of protein adsorption.
a: Protein adsorption on hydrophobic surface.
b: Protein adsorption on MPC-coated surface.

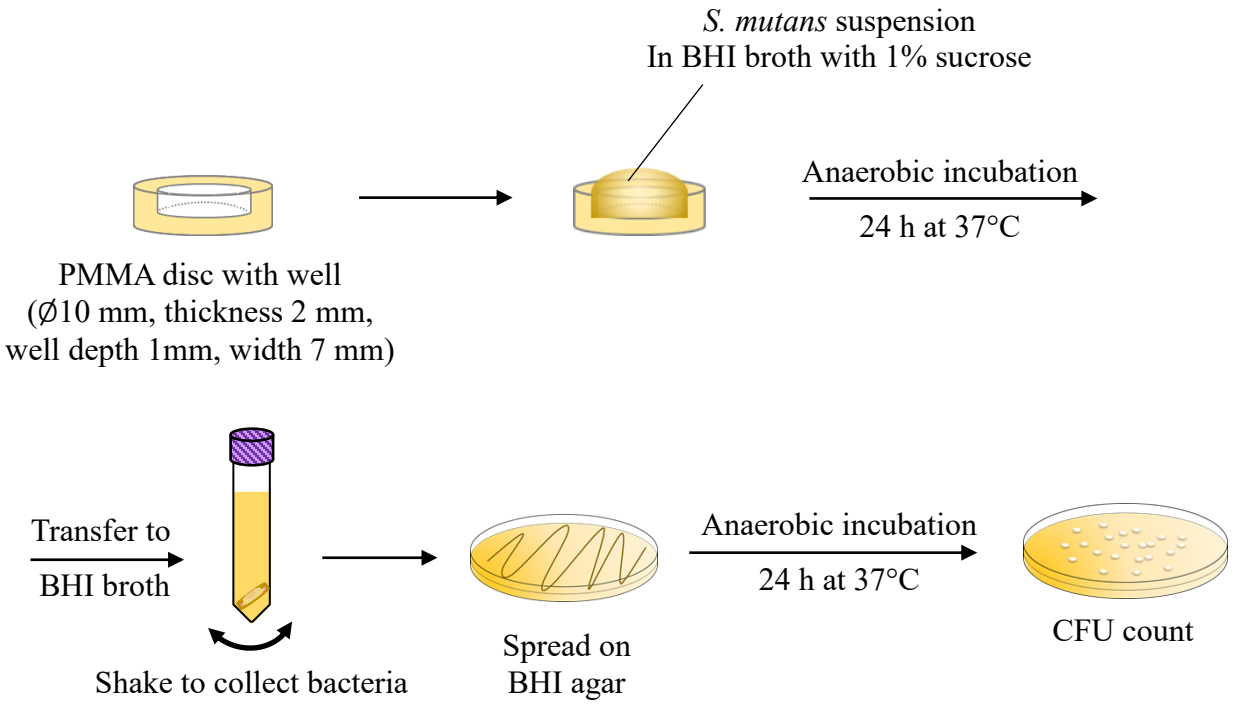

Figure 11. Procedure of on-disc culture assay.

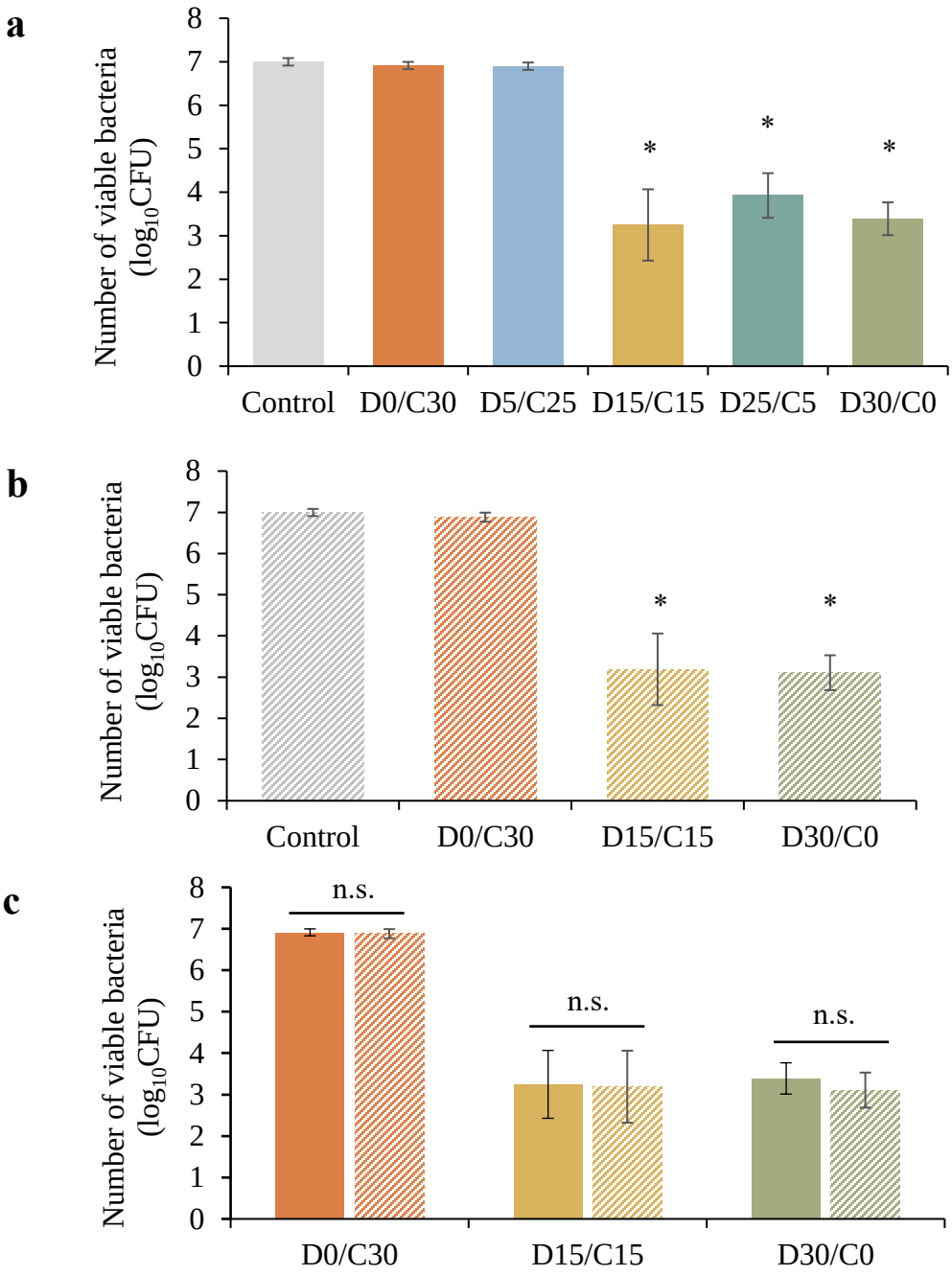

Figure 12. Number of *S. mutans* after incubation on copolymer coated disc with well for 24 h.

a: Before 28-day immersion in water.

b: After 28-day immersion in water.

c: Comparison between before and after 28-day immersion in water.

Hatched bar represents the number of *S. mutans* on the coated disc after immersion. The error bar represents the standard deviation. Asterisks represent statistically significant difference from control (ANOVA, Tukey's HSD test, $p < .05$, n = 5). 'n.s.' denotes no significant difference between two groups. (Student's *t*-test, $p > .05$, n=5).

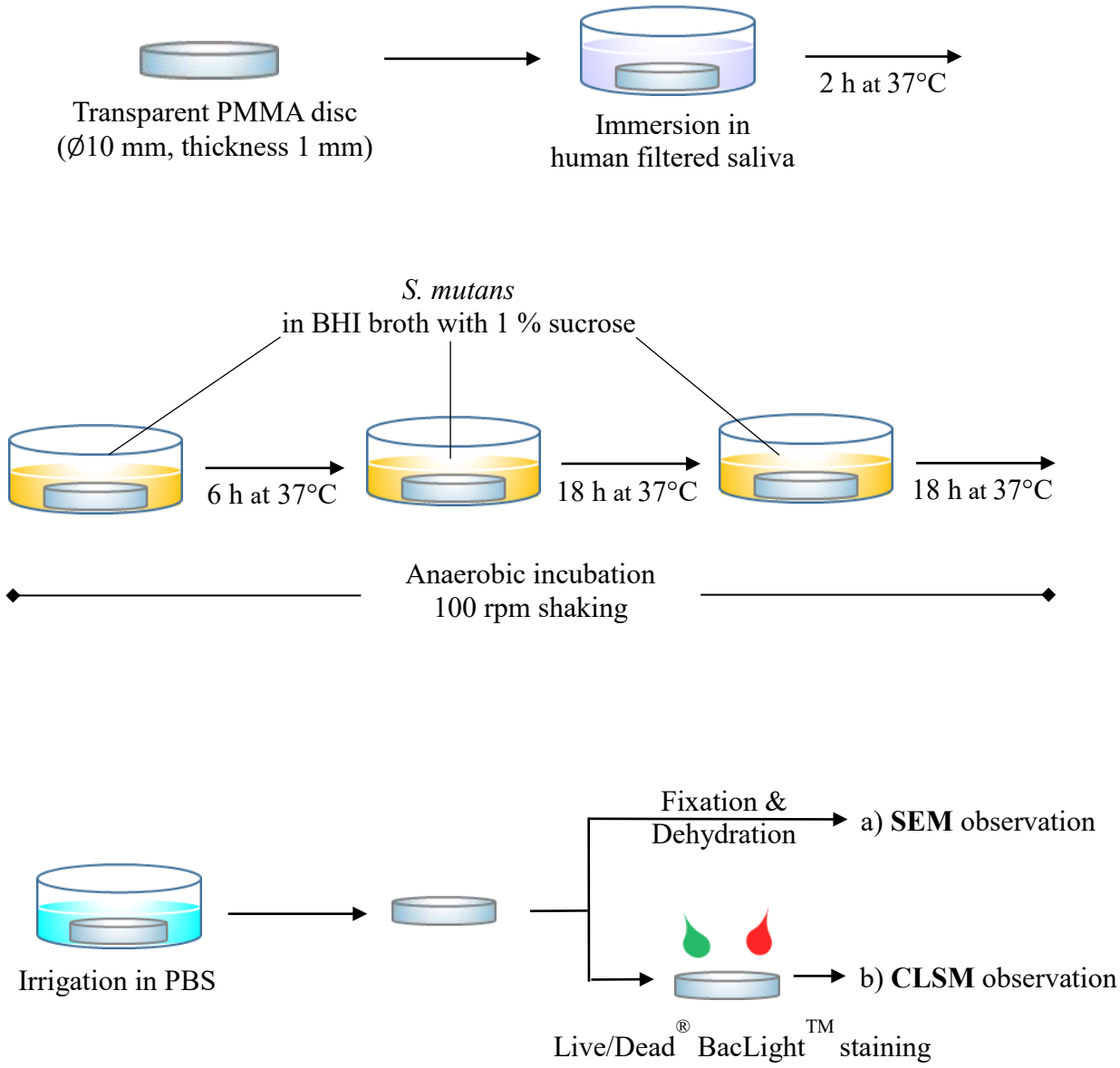

Figure 13. Procedure of biofilm formation test.

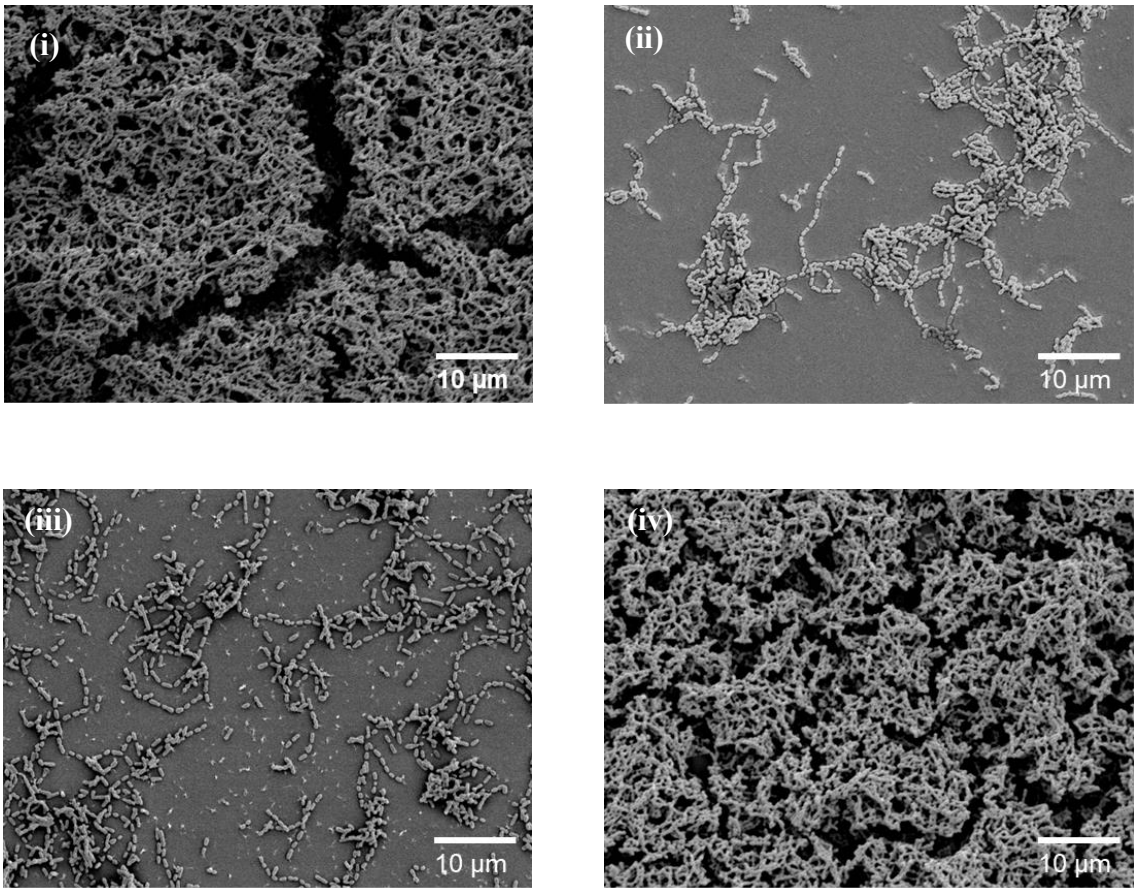

Figure 14. SEM images of *S. mutans* biofilm formed after 48-hour incubation on the surface of coated specimen.

i) Control, ii) D0/C30, iii) D15/C15, and (iv) D30/C0.

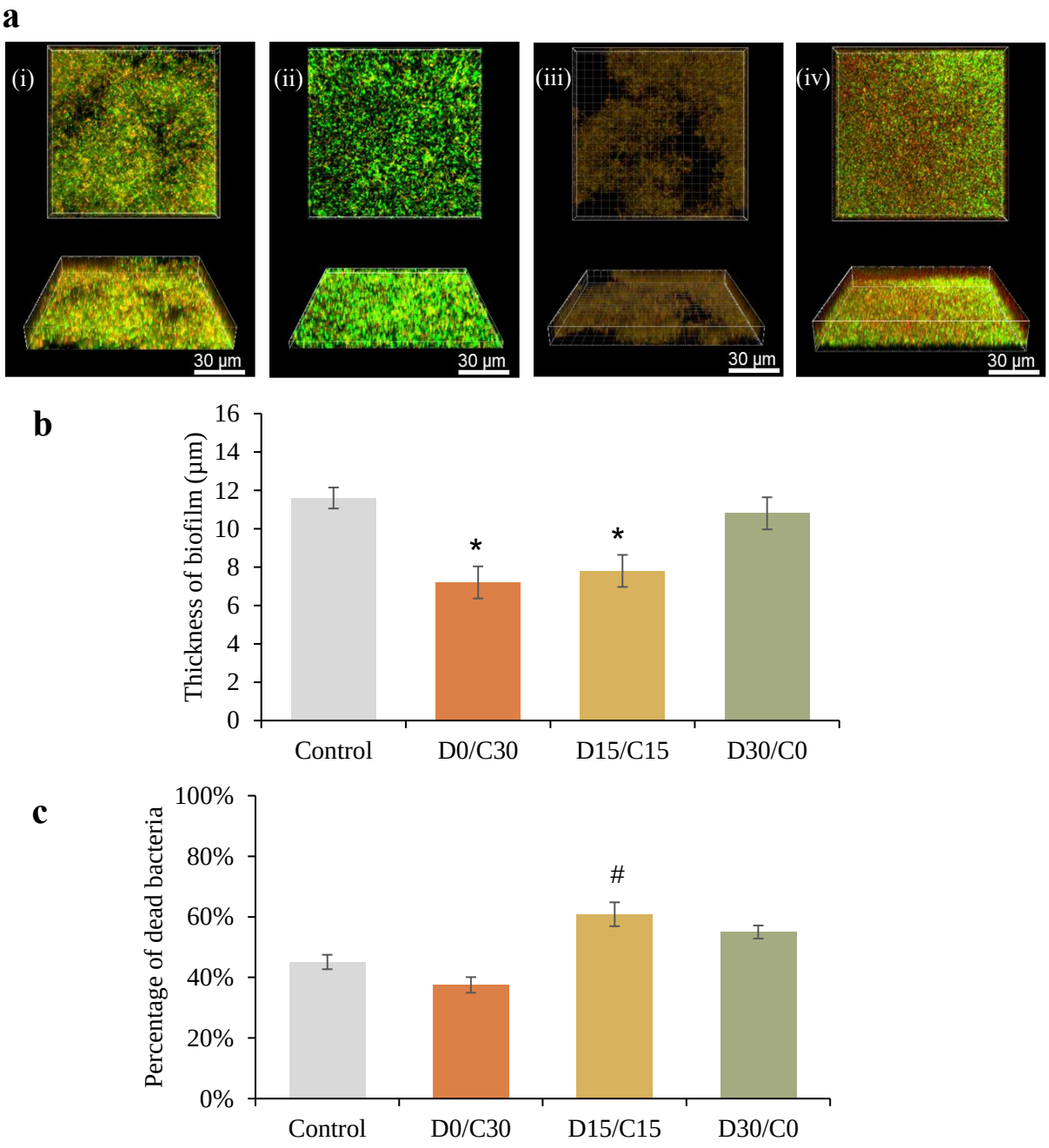

Figure 15. *S. mutans* biofilm formation after 48-hour incubation on the surface of coated specimen.

a: CLSM images i) Control, ii) D0/C30, iii) D15/C15, and iv) D30/C0.

b: Thickness of biofilm analyzed from CLSM images. Asterisks represent statistically significant difference from control (ANOVA, Tukey's HSD test, $p < .05$, n = 5).

c: Percentage of dead bacteria analyzed from CLSM images. Hashtag represents statistically significant increase from control (ANOVA, Tukey's HSD test, $p < .05$, n = 3).

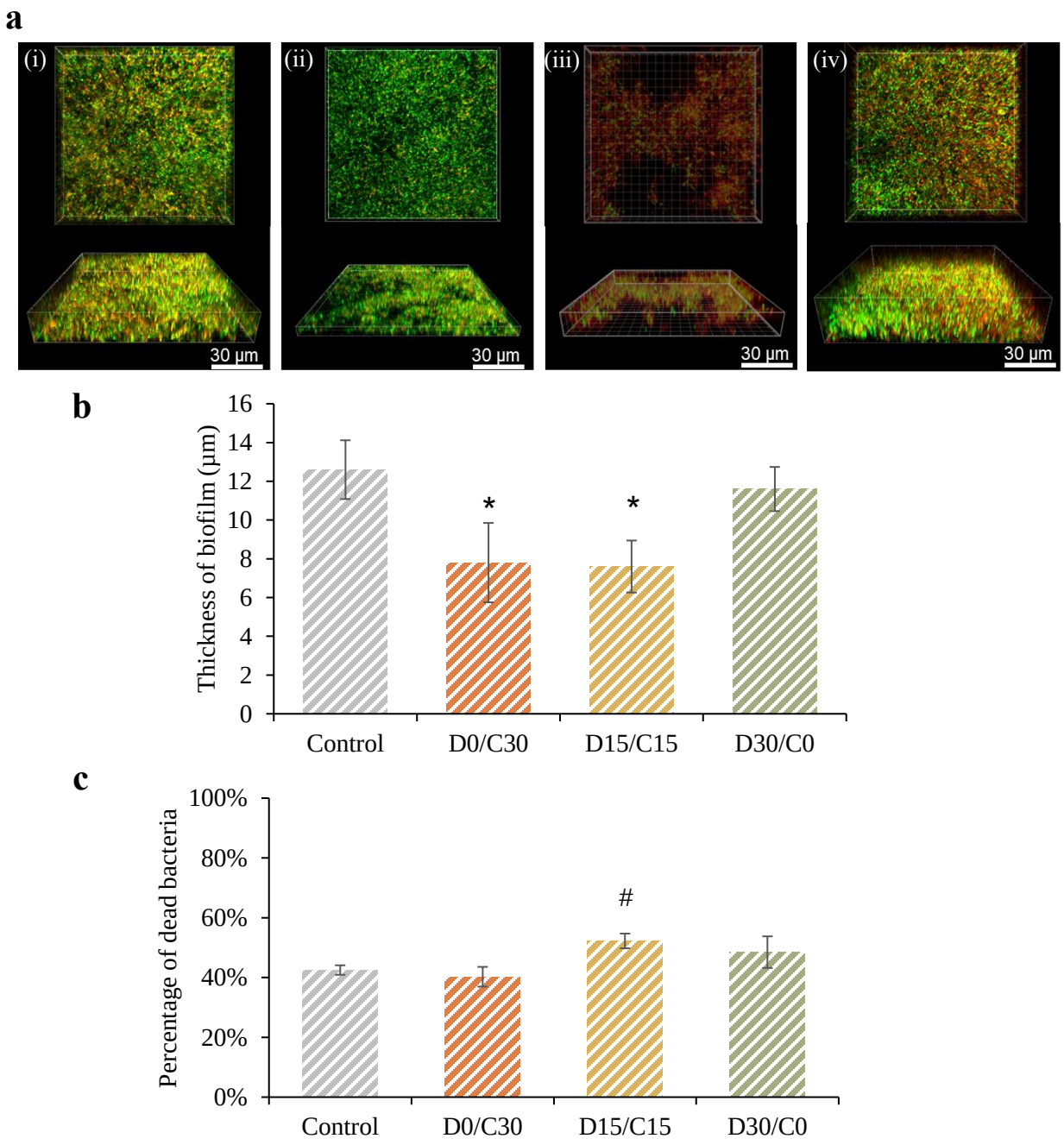

Figure 16. *S. mutans* biofilm formation after 48-hour incubation on the surface of coated specimen with ageing.

a: CLSM images i) Control, ii) D0/C30, iii) D15/C15, and iv) D30/C0.

b: Thickness of biofilm analyzed from CLSM images. Asterisks represent statistically significant difference from control (ANOVA, Tukey's HSD test, $p < .05$, n = 5).

c: Percentage of dead bacteria analyzed from CLSM images. Hashtag represents statistically significant increase from control (ANOVA, Tukey's HSD test, $p < .05$, n = 3).

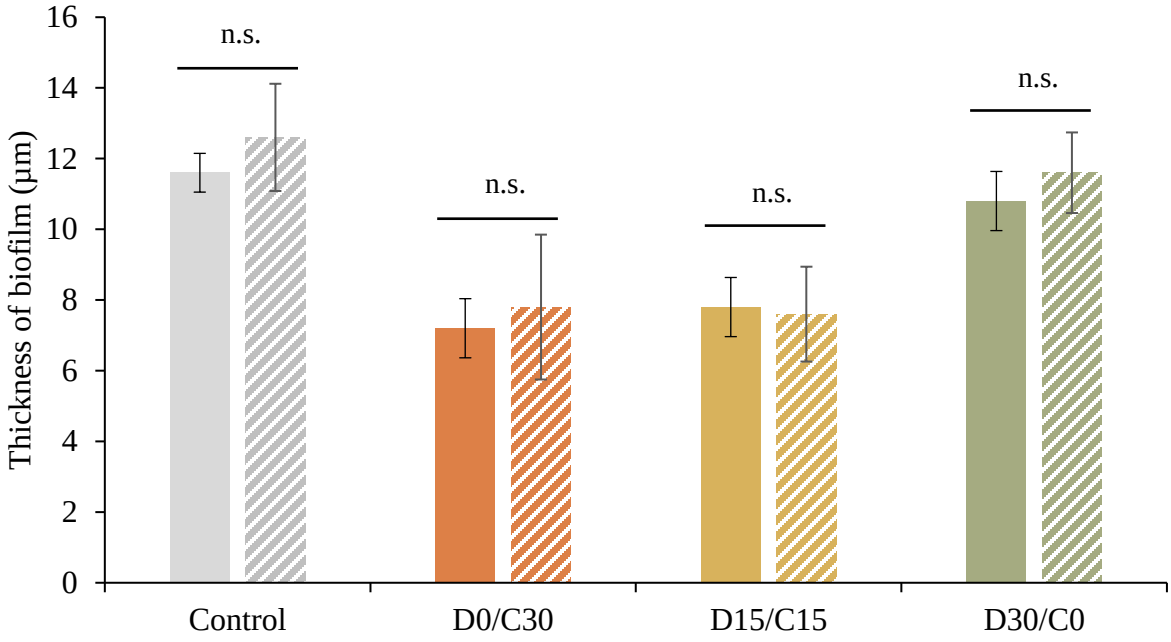

Figure 17. Comparison of the thickness of biofilm analyzed from CLSM images before and after 28-day immersion of the specimen.
The error bar represents the standard deviation. Hatched bars represent the data after 28-day immersion. 'n.s.' denotes no significant difference between two groups. (Student's *t*-test, $p > .05$, n = 5).

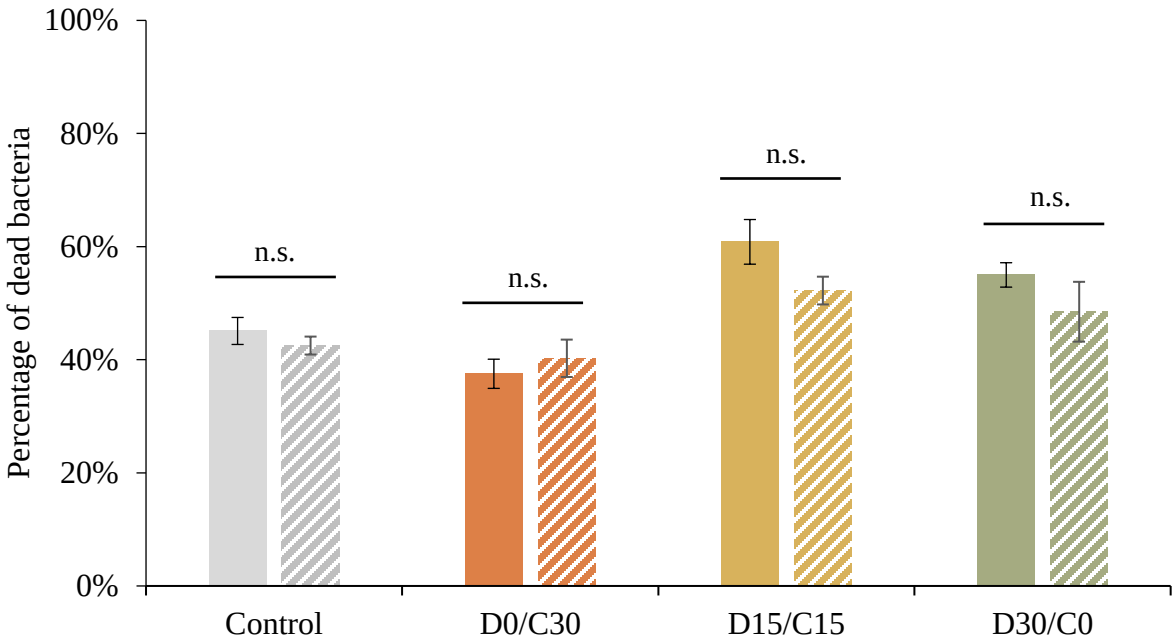

Figure 18. Comparison of the percentage of dead bacteria analyzed from CLSM images before and after 28-day immersion of the specimen.

Plain bars represent dead bacteria. Hatched bars represent the data after 28-day immersion. 'n.s.' denotes no significant difference between two groups. (Student's *t*-test, $p > .05$, n = 3).

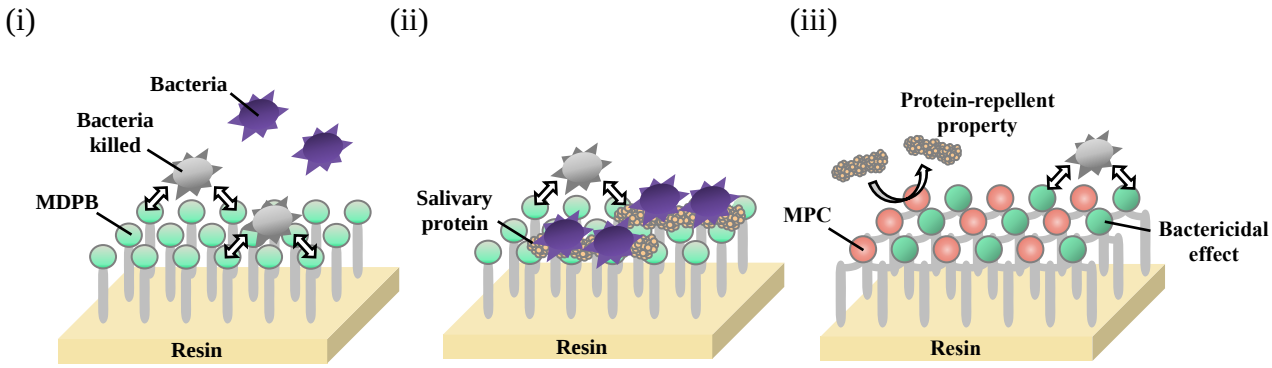

Figure 19. Scheme of dual functions of protein repellency and antibacterial effect. (i) Dental resins with immobilized MDPB exhibit antibacterial effects, which depend on the contact inhibition of bacteria. (ii) However, their effectiveness can be readily reduced by coverage with salivary protein. (iii) The novel surface coating composed of MDPB and MPC exhibits protein repellent ability and bactericidal effect.